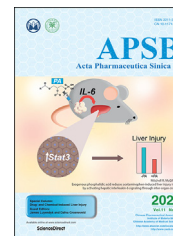




Chinese Pharmaceutical Association
Institute of Materia Medica, Chinese Academy of Medical Sciences

Acta Pharmaceutica Sinica B

www.elsevier.com/locate/apsb
www.sciencedirect.com



REVIEW

Antibody–drug conjugates: Recent advances in linker chemistry



Zheng Su^{a,b,†}, Dian Xiao^{b,†}, Fei Xie^b, Lianqi Liu^b, Yanming Wang^b,
Shiyong Fan^{b,*}, Xinbo Zhou^{b,*}, Song Li^{a,b}

^aSchool of Pharmaceutical Engineering, Shenyang Pharmaceutical University, Shenyang 110016, China

^bNational Engineering Research Center for the Emergency Drug, Beijing Institute of Pharmacology and Toxicology, Beijing 100850, China

Received 18 January 2021; received in revised form 17 March 2021; accepted 26 March 2021

KEY WORDS

Antibody–drug conjugate;
Linker;
Chemical trigger;
Linker–antibody attachment;
Linker–payload attachment

Abstract Antibody–drug conjugates (ADCs) are gradually revolutionizing clinical cancer therapy. The antibody–drug conjugate linker molecule determines both the efficacy and the adverse effects, and so has a major influence on the fate of ADCs. An ideal linker should be stable in the circulatory system and release the cytotoxic payload specifically in the tumor. However, existing linkers often release payloads nonspecifically and inevitably lead to off-target toxicity. This defect is becoming an increasingly important factor that restricts the development of ADCs. The pursuit of ADCs with optimal therapeutic windows has resulted in remarkable progress in the discovery and development of novel linkers. The present review summarizes the advance of the chemical trigger, linker–antibody attachment and linker–payload attachment over the last 5 years, and describes the ADMET properties of ADCs. This work also helps clarify future developmental directions for the linkers.

© 2021 Chinese Pharmaceutical Association and Institute of Materia Medica, Chinese Academy of Medical Sciences. Production and hosting by Elsevier B.V. This is an open access article under the CC BY-NC-ND license (<http://creativecommons.org/licenses/by-nc-nd/4.0/>).

*Corresponding author. Tel: +86 10 66930603 (Shiyong Fan), +86 10 66930673 (Xinbo Zhou).

E-mail addresses: fsyn1996@163.com (Shiyong Fan), zhouxinbo@bmi.ac.cn (Xinbo Zhou).

[†]These authors made equal contributions to this work.

Peer review under responsibility of Chinese Pharmaceutical Association and Institute of Materia Medica, Chinese Academy of Medical Sciences.

<https://doi.org/10.1016/j.apsb.2021.03.042>

2211-3835 © 2021 Chinese Pharmaceutical Association and Institute of Materia Medica, Chinese Academy of Medical Sciences. Production and hosting by Elsevier B.V. This is an open access article under the CC BY-NC-ND license (<http://creativecommons.org/licenses/by-nc-nd/4.0/>).

1. Introduction

Antibody–drug conjugate (ADC), comprising a monoclonal antibody (mAb), the cytotoxic payload and the linker, has developed rapidly in recent years and is gradually revolutionizing clinical cancer therapy. This technology appeared a century ago¹, but it is becoming mature in the past 5 years. Currently, 10 ADCs have been approved and more than 80 ADCs are at different phases of clinical trials^{2–8}.

The linker connects the antibody and the cytotoxic payload and is a key component in the function of ADCs. The linker imparts the following characteristics to ADCs: (1) high stability in the circulation, and (2) specific release of payload in the target tissue. These seemingly contradictory requirements of stability and release lead to the major challenge in the development of linkers. To achieve the above requirement, various linkers have been developed and can be divided into two types according to their cleavage method. The first type is the cleavable linker, which has a chemical trigger in its structure that can be efficiently cleaved to release the cytotoxic payload in the tumor. More than 80% of the clinically approved ADCs employ cleavable linkers⁹, such as inotuzumab ozogamicin (Besponsa) and brentuximab vedotin (Adcetris)^{10,11}. The other type of linker is noncleavable. In contrast to the cleavable linker, there are no chemical triggers in this structure, and the linker is part of the payload. This type of linker has been employed only in adotrastuzumab emtansine (Kadcyla, T-DM1) among the approved ADCs¹².

Although ADCs have achieved great success, future development is increasingly constrained by the linkers. The defects of the classical linkers employed in the marketed ADCs include the following aspects: (1) the nonspecific release of payloads in non-tumorous tissues, leading to off-target toxicity and a limited therapeutic window. The most notable case is that of gemtuzumab ozogamicin (Mylotarg) developed by Pfizer. It was withdrawn in 2010 for causing severe liver toxicity due to an unstable *N*-acyl-hydrazone linker¹³. Although Mylotarg was approved again in 2017 after redesign, the U.S. Food and Drug Administration (FDA) required a black-box warning for the potential of liver toxicity. (2) The retro-Michael elimination reaction of the commonly-used maleimide attachment leads to reduced efficacy of ADCs. For instance, the classic succinimidyl 4-(*N*-maleimidomethyl) cyclohexane-1-carboxylate (SMCC) linker

degrades to 38% after 120 h in mice plasma, and Kadcyla containing an SMCC linker exhibited a 29% drug-to-antibody ratio (DAR) decrease in mice after 7 days^{14–16}. (3) The limited linker–payload attachment is insufficient for the rapid expansion of payloads. Novel ADCs have developed rapidly to treat cancer, microbial infection¹⁷, and immune modulation¹⁸. Many newly designed payloads are awaiting appropriate linker–payload attachments.

To solve the above problems, there have been important developments in linker design in the past 5 years, which are as follows (Fig. 1): (1) the optimization of the existing chemical triggers and development of novel chemical triggers to generate highly selective linkers; (2) the development of novel linker–antibody attachments to produce stable and homogeneous ADCs; (3) the development of additional linker–payload attachments to allow the expansion of payloads; (4) the optimization of linkers to improve the absorption, distribution, metabolism, and excretion (ADME) of ADCs. Therefore, a literature review initially based on the 3 components of linkers was carried out to provide a comprehensive overview of the developments over the past 5 years with regard to the above four aspects.

2. Chemical triggers of the linker

The chemical triggers, which control the release of the payloads, are the most important part of linkers. The most serious challenge in their development is the undesired nonspecific release of payloads in normal tissues, which can lead to off-target toxicity. For instance, the dipeptide triggers, which are classical chemical triggers and employed in more than 40 ADCs in clinical use, can be cleaved by cathepsin. Cathepsin is nonspecifically expressed in all tissues, so when the ADCs are taken up into normal tissue with the targeted antigen expression, the dipeptide triggers are activated to release the toxic payloads, leading to adverse effects. To obtain higher selectivity, many novel triggers have been developed over the past 5 years. With current cleavage strategies the chemical triggers can be divided into cathepsin-cleavable triggers, acid-cleavable triggers, GSH-cleavable triggers, Fe(II)-cleavable trigger, novel enzyme-cleavable triggers, photo-responsive-cleavable triggers, and bioorthogonal cleavable triggers (Table 1). Among them, cathepsin-cleavable triggers, GSH-cleavable triggers, and acid-cleavable triggers have been well studied and employed in approved ADCs. Other novel cleavable triggers are

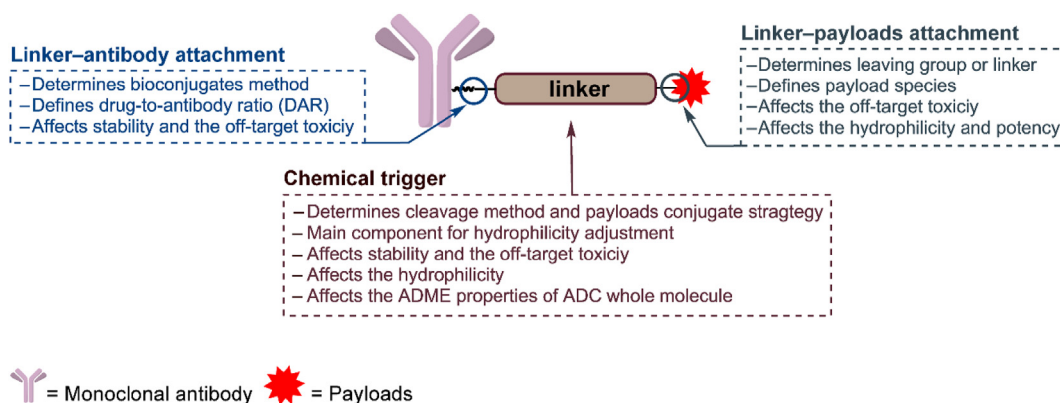


Figure 1 The general structure of an ADC and the roles of the chemical trigger, the linker–antibody attachment and the linker–payload attachment.

Table 1 Chemical triggers described in this review.

| Chemical trigger | Structure | Mechanism | Payload | Ref. |
|-------------------------------------|---|--|----------------|------|
| Acid cleavable triggers | Hydrazone trigger | Linkers cleavage by low pH of tumor acidic microenvironment or lysosomes | Calicheamicin | 10 |
| | Carbonate trigger | | SN-38 | 27 |
| | Silyl ether trigger | | MMAE | 28 |
| GSH cleavable trigger | Disulfide trigger | Linkers cleavage by high level of GSH in cytoplasm | DM1, DM3, MMAE | 30 |
| Fe(II) cleavable trigger | 1,2,4-Trioxolane trigger | Linker cleavage by elevating levels of ferrous iron | PBD | 31 |
| | | | MMAE | 34 |
| Cathepsin cleavable triggers | Dipeptide trigger | Linkers cleavage by cathepsin in lysosomes | MMAE, DM1 | 21 |
| | Triglycyl (CX) trigger | | DM1 | 22 |
| | cBu-Cit trigger | | MMAE, PBD | 20 |
| Glycosidase cleavable triggers | β -Glucuronide trigger | Linkers cleavage by β -glucuronidase in lysosomes | MMAE | 35 |
| | β -Galactoside trigger | Linkers cleavage by β -galactosidase in lysosomes | MMAE | 36 |
| Phosphatase cleavable triggers | Pyrophosphate trigger | Linkers cleavage by phosphatase and pyrophosphates in lysosomes | Budesonide | 18 |
| Sulfatase cleavable trigger | Arylsulfate trigger | Linkers cleavage by sulfatase in lysosomes | MMAE | 37 |
| Photo-responsive cleavable triggers | Heptamethine cyanine fluorophore trigger | Linkers cleavage by irradiation with NIR light ($\lambda = 650\text{--}900\text{ nm}$) | CA-4 | 46 |
| | <i>O</i> -Nitrobenzyl trigger | Linkers cleavage by irradiation with UV light ($\lambda = 365\text{ nm}$) | MMAE | 47 |
| | PC4AP trigger | Linkers cleavage both by irradiation with near-infrared (NIR) light ($\lambda = 365\text{ nm}$) and intramolecular addition reaction with nearby amine | DOX | 48 |
| Bioorthogonal cleavable trigger | dsProc trigger | Linkers cleavage by the bioorthogonal cleavage pair: Cu(I)-BTAA/dsProc | DOX | 55 |
| Non-cleavable linkers | MD linker | No linker cleavage, ADCs metabolizes amino acid appendage, a linker and molecule cytotoxicity upon entry lysosome | TRMRA | 14 |
| | PEG linkers with intermediates of alkyne, triazole and piperazine | | PBD Dimer | 58 |
| | Mal-PAB linker | | MMAE | 59 |

designed for selective cleavage in cancer cells to decrease their off-target toxicity from nonspecific uptake. In addition, novel noncleavable linkers also have been introduced.

2.1. Cathepsin cleavable triggers

In 2017 Caculitan et al.¹⁹ discovered that the valine-citrulline (Val-Cit) linker exhibited widespread sensitivity to a variety of cathepsins, including cathepsin B, cathepsin K, cathepsin L, etc. This could be detrimental, as only cathepsin B is thought to be highly expressed in cancer cells, and the widespread sensitivity to other cathepsins could induce off-target toxicity in normal cells. Wei et al.²⁰ designed a linker that used a cyclobutane-1,1-dicarboxamide (cBu) structure that was predominantly dependent on cathepsin B (Fig. 2A). In intracellular cleavage studies, drug release from cBu-Cit-containing linkers was efficiently suppressed by a cathepsin B inhibitor (over 75%), while a cathepsin K inhibitor did not have a significant effect. Conversely, the traditional Val-Cit-containing linker appeared strongly resistant to all single-protease inhibitors (inhibitors of cathepsins B, L, and K, all less than 15%). Meanwhile the cBu-Cit-containing linkers exhibited a maximum velocity/Michaelis constant (V_{\max}/K_m) like that of the Val-Cit containing linker. Compared with Val-Cit linker-containing ADCs, cBu-Cit linker-containing ADCs exhibited equally potent antiproliferation effects *in vitro*, and both

ADCs were efficacious in inhibiting tumor growth at the dose of 3 mg/kg, but the cBu-Cit linker-containing ADCs exhibited greater tumor suppression.

In 2016 Dorywalska et al.²¹ confirmed that carboxylesterase 1C (Ces1C) is the enzyme that leads to the instability of Val-containing peptide linkers in mouse plasma. The Val-Cit-containing ADC was highly stable in Ces1C-knockout mice. Based on the versatility and importance of xenograft mouse models in ADC preclinical research, it is important to design peptide linkers that are stable in mouse models. Singh et al. designed a triglycyl peptide linker (CX) for ADCs with maytansinoid (DM1) as the payload (Fig. 2B)²². This linker consisted of three glycyl residues and showed extremely high stability in mouse plasma. In a pharmacokinetics study, the CX-DM1-containing ADCs exhibited stability comparable to that of SMCC-DM1-containing ADCs; for instance, half-life ($t_{1/2}$) values of 9.9 vs. 10.4 days, clearance (CL) values of 0.7 vs. 0.7 mL/h/kg, and area under the curve ($AUC_{0\rightarrow\infty}$) values of 15,225 vs. 14,370 h·mg/mL, respectively. Furthermore, the *in vitro* cytotoxicity of the CX linker-containing ADCs was significantly improved compared with that of the SMCC-DM1-based ADCs. Similar data were obtained in the *in vivo* experiments; the CX-DM1-containing ADCs, even at 3 mg/kg, were more active than a 15 mg/kg dose of the SMCC-DM1 ADCs. Surprisingly, the CX-DM1-containing ADCs possessed higher *in vivo* activity and a 50-

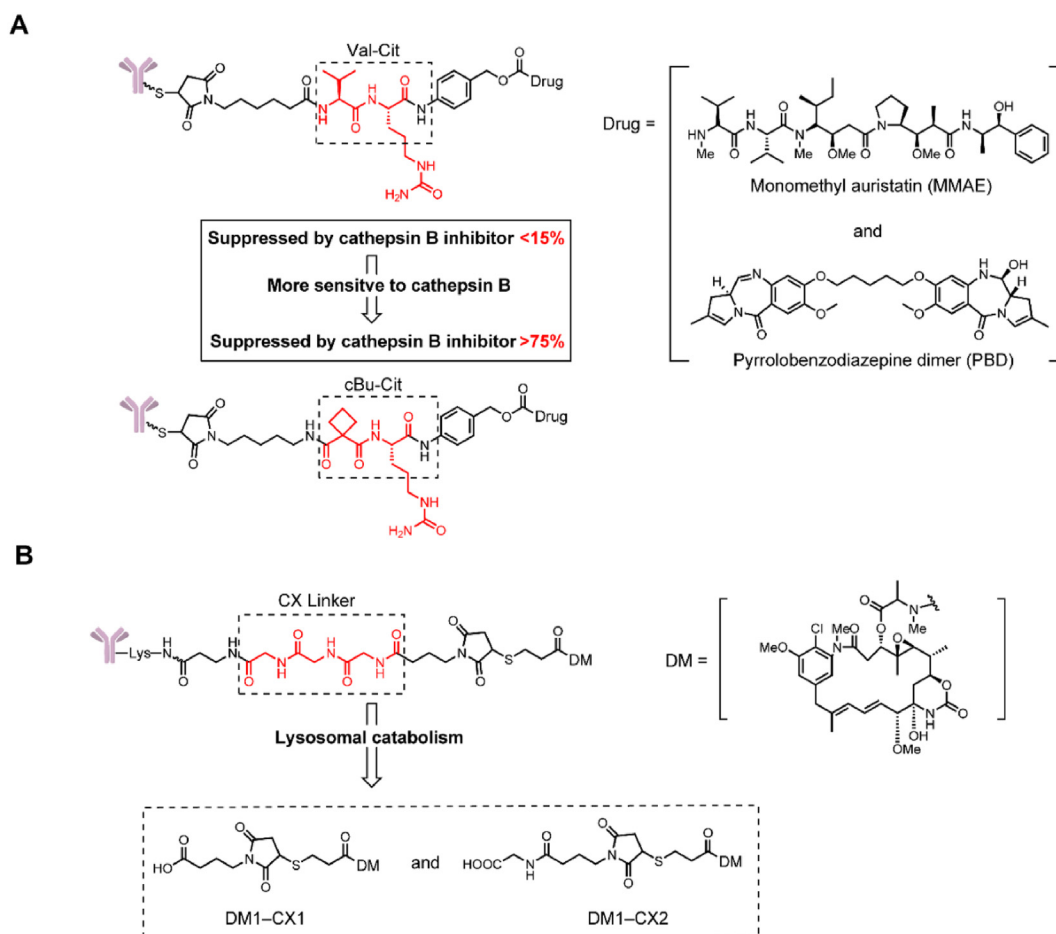


Figure 2 Structures of cathepsin-cleavable triggers. (A) The structure of the cBu-Cit-PABC-containing ADCs. Adapted with modification from Ref. 19 © 2017 American Association for Cancer Research. (B) The structure of CX-containing ADCs and catabolites expected from lysosomal proteolysis. Adapted with modification from Ref. 21 © 2016 American Association for Cancer Research.

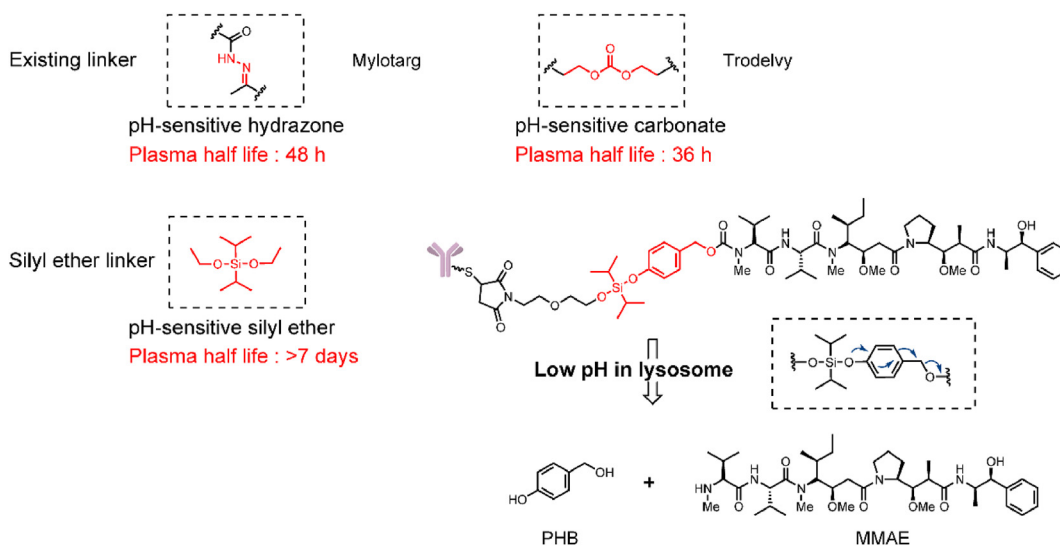


Figure 3 Approved acid-cleavable linker-containing ADCs and the structure of silyl ether-containing ADC. Adapted with modification from Ref. 28 © 2019 Multidisciplinary Digital Publishing Institute.

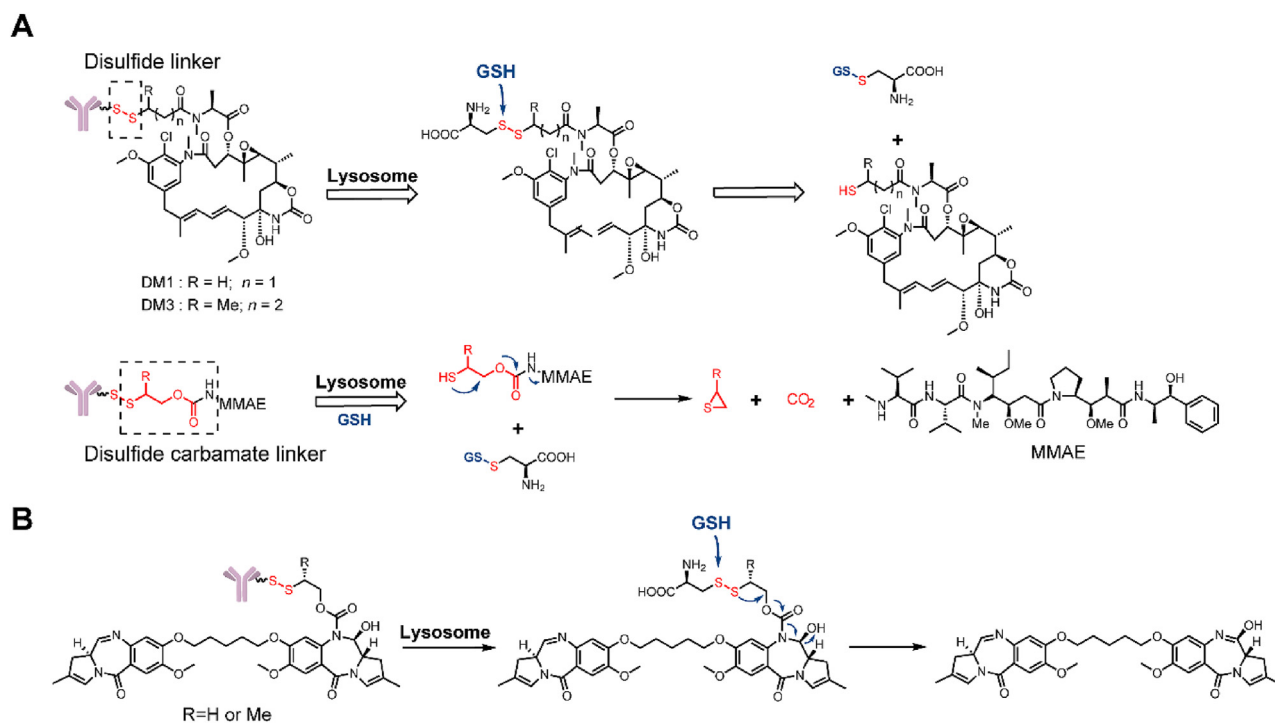


Figure 4 Structures of GSH-cleavable triggers. (A) The structure and release mechanism of an ADC containing a disulfide linker and a disulfide-carbamate linker. Adapted with modification from Ref. 30 © 2017 Royal Society of Chemistry. (B) The structure and release mechanism of an ADC containing a disulfide-carbamate linker with a PBD-dimer. Adapted with modification from Ref. 31 © 2017 American Association for Cancer Research.

fold higher preclinical therapeutic index [maximum tolerated dose/minimum effective dose (MTD/MED) ratio] than SMCC-DM1-containing ADCs in both the EGFR and EpCAM xenograft mouse models.

The optimization of peptide linkers is not limited to developing novel structures. Peptide linkers can be optimized by minimal structural changes, including the types and stereochemistry of the amino acids. Our group demonstrated that valine-alanine (Val-Ala) has better hydrophilicity and stability than Val-Cit²³. While the two ADCs had an average DAR of approximately 7, the Val-Ala-based ADCs had no obvious increase in the dimeric peak. However, the aggregation of Val-Cit-based ADCs increased to 1.80%. In stereochemical studies, Reid et al.²⁴ and Salomon et al.²⁵ both indicated that ADCs containing an (L,L) dipeptide linker showed higher antitumor activity *in vitro* and *in vivo* than other amino acid configurations.

2.2. Acid-cleavable triggers

Acid-cleavable linkers utilize the pH difference between tumor tissue (4.0–5.0) and plasma (~7.4) to selectively release payloads into tumor tissues²⁶. This strategy yielded the earliest clinical success with Mylotarg and was later employed in Besponsa^{2,10}. However, the insufficient stability of acid-cleavable linkers severely limits their application in ADCs, and a phenylketone-derived hydrazone linker was hydrolyzed with a $t_{1/2} = 2$ days in human and mouse plasma. The serum stability of the Sacituzumab govitecan (Trodelvy), which contains acid-cleavable carbonate linkers, was also unsatisfactory with a $t_{1/2} = 36$ h²⁷. Accordingly, acid-cleavable ADCs require more stable linkers or must employ only moderately cytotoxic payloads.

In 2019, our group developed a novel silyl ether-based acid-cleavable ADC carrying highly cytotoxic monomethyl auristatin E (MMAE, Fig. 3)²⁸. This design greatly improved the stability of the acid-cleavable linker and should be sufficient to support acid-cleavable ADCs containing highly cytotoxic payloads. Compared with the traditional hydrazine linker ($t_{1/2} = 2$ days) and carbonate linker ($t_{1/2} = 36$ h), the $t_{1/2}$ of the novel silyl ether linker-MMAE conjugate was more than 7 days in human plasma. This novel ADC containing a silyl ether linker possessed strong cell inhibitory activity (HER2⁺ cell lines, IC₅₀ = 0.028–0.170 nmol/L) and exhibited a better therapeutic effect than monoclonal antibodies in a mouse xenograft model.

2.3. Glutathione (GSH)-cleavable triggers

Glutathione (GSH)-cleavable triggers rely on the higher level of glutathione in the cytoplasm (1–10 mmol/L) compared to the blood plasma (~5 μmol/L)²⁹. Disulfide bonds are most commonly used in these triggers. However, the present disulfide bond constructs cannot achieve a perfect combination of high circulatory stability and efficient intracellular release. In 2017, Thomas et al.³⁰ tried to solve this problem by attaching the small molecule drug directly to engineered cysteines in a THIOMAB antibody (Fig. 4A). By connecting directly to the antibody, a steric protection from the antibody would increase the circulatory stability. Firstly, by screening sites for conjugation, they identified that LC-K149C as a stable conjugation site for disulfide. *In vivo* stability study showed that when DM1 was attached through a disulfide to K149C, more than 50% of the drug remained attached even after seven days. An *in vivo* efficacy study showed that this novel anti-CD22-DM1-ADC could induce tumor regression at a

single dose of 3 mg/kg in a human lymphoma tumor xenograft mouse model. Furthermore, this novel Cys-linked disulfide-conjugation strategy could also be applied to non-thiol payloads, such as MMAE, by inserting a self-cleaving disulfide linker. In the same year, this novel strategy was used to prepare ADCs armed with a PBD as a payload (Fig. 4B)³¹. Compared with the malimide peptide (Val-Cit)-PBD-ADC, the novel disulfide ADC exhibited similar activity at several doses in a human non-Hodgkin lymphoma tumor xenograft mouse model. At the same time, this novel disulfide-ADC had a higher MTD than that of a Val-Cit-ADC (10 vs. 2.5 mg/kg). In conclusion, these results demonstrate the potential for novel linkers to improve the biophysical properties and increase the therapeutic index of ADCs.

2.4. Fe(II) cleavable trigger

Abnormal iron metabolism can elevate the levels of unbound ferrous iron³². Based on this strategy, increasing the unbound ferrous iron concentration has been utilized in prodrug design³³. In 2018, Spangler et al.³⁴ reported an Fe(II)-reactive 1,2,4-trioxolane scaffold (TRX) linker and initially employed this cleavage method with ADCs (Fig. 5A). The linker was cleaved by a Fenton reaction between the O—O bond of TRX and Fe(II), affording a carbonyl intermediate and releasing the payload via β -elimination (Fig. 5B). In an *in vitro* cytotoxicity study, the TRX linker-containing ADCs demonstrated activity in antigen positive cells (EC_{50} = 0.07 nmol/L) similar to that of classic Val-Cit linker-containing ADCs. However, the TRX linker-containing ADCs still showed significant toxicity (EC_{50} = 0.61 nmol/L) in the antigen-negative MDA-MB-468 cell lines. This instability was caused by the nonspecific interaction between the adamantane moiety and the nearby sites on the antibody, resulting in trioxolane heterolytic ring cleavage. The researchers intended to avoid this reaction in the ADCs by the addition of inert polyethylene glycol (PEG) spacers between the antibody and adamantane.

2.5. Novel enzyme-cleavable triggers

In addition to the classic β -glucuronidase-cleavable linkers that were developed for ADCs in 2006³⁵, β -galactosidase was

discovered to be overexpressed in tumor cells and possess hydrolytic activity. In 2017, Kolodych et al.³⁶ described a β -galactosidase-cleavable linker-containing ADCs (Fig. 6A). The ADCs containing this β -galactosidase-cleavable linker was rapidly hydrolyzed *in vitro* at 10 U/mL β -galactosidase (Fig. 6B). The ADC comprising trastuzumab and MMAE via this linker exhibited a lower IC_{50} (8.8 pmol/L) than that of ADC containing a Val-Cit linker (14.3 pmol/L) and Kadcykla (33 pmol/L). Equivalent results were obtained with *in vivo* experiments; ADCs containing the β -galactosidase-cleavable linker exhibited a 57% and 58% reduction in tumor volumes in a xenograft mouse model at a single dose of 1 mg/kg, but the efficiency of Kadcykla was not statistically significant at the same dose. In addition, the novel ADCs showed a higher reduction of tumor growth than Kadcykla through a Principal Components Analysis (PCA).

In 2020, a sulfatase-cleavable linker was described by Bargh et al.³⁷ (Fig. 6C). Sulfatase, which is analogous to β -galactosidase, is a hydrolytic enzyme overexpressed in tumor cells. The sulfatase-cleavable linker exhibited definite susceptibility to sulfatase enzymes ($t_{1/2}$ = 24 min) in a release study. In mouse plasma, compared with Val-Ala and Val-Cit linker conjugates hydrolyzed within 1 h, sulfatase-cleavable linker conjugates demonstrated high plasma stability (over 7 days). Compared with the *in vitro* cytotoxicity of noncleavable ADCs (IC_{50} = 609 pmol/L) and Val-Ala containing ADCs (IC_{50} = 92 pmol/L), sulfatase-linker-containing ADCs exhibited higher cytotoxicity (IC_{50} = 61 and 111 pmol/L) and a superior selectivity in HER2⁺ cells.

Phosphate and pyrophosphate groups can markedly improve the hydrophilicity of linkers and can be employed to load lipotropic payloads. In 2016, Kern et al.³⁸ employed a terminal phosphate/pyrophosphate as both a leaving group and hydrophilic group for the Val-Cit-*p*-aminobenzoyloxycarbonyl (PAB) linker with the highly lipophilic glucocorticoid budesonide (Fig. 7A). However, the $t_{1/2}$ in the plasma was less than 6 h, which failed to meet the stability requirement of ADCs. Subsequently, budesonide phosphate could be detected, suggesting that payload release may occur in two steps by cathepsin and phosphatase. The double sensitivity to cathepsin and phosphatase may be responsible for the instability of the linker. While the specific hydrolysis mechanism was not confirmed, it was proven

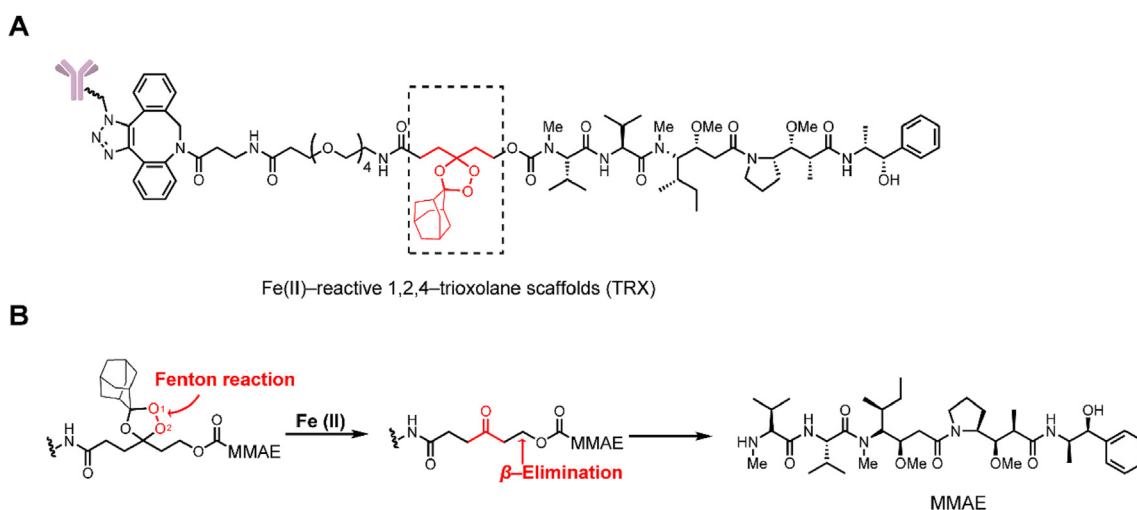


Figure 5 Structures of Fe(II)-cleavable trigger. (A) The structure of the Fe(II)-reactive (TRX) linker-containing ADC. Adapted with modification from Ref. 34 © 2018 American Chemical Society. (B) Release mechanism of Fe(II)-cleavable linker-containing ADCs.

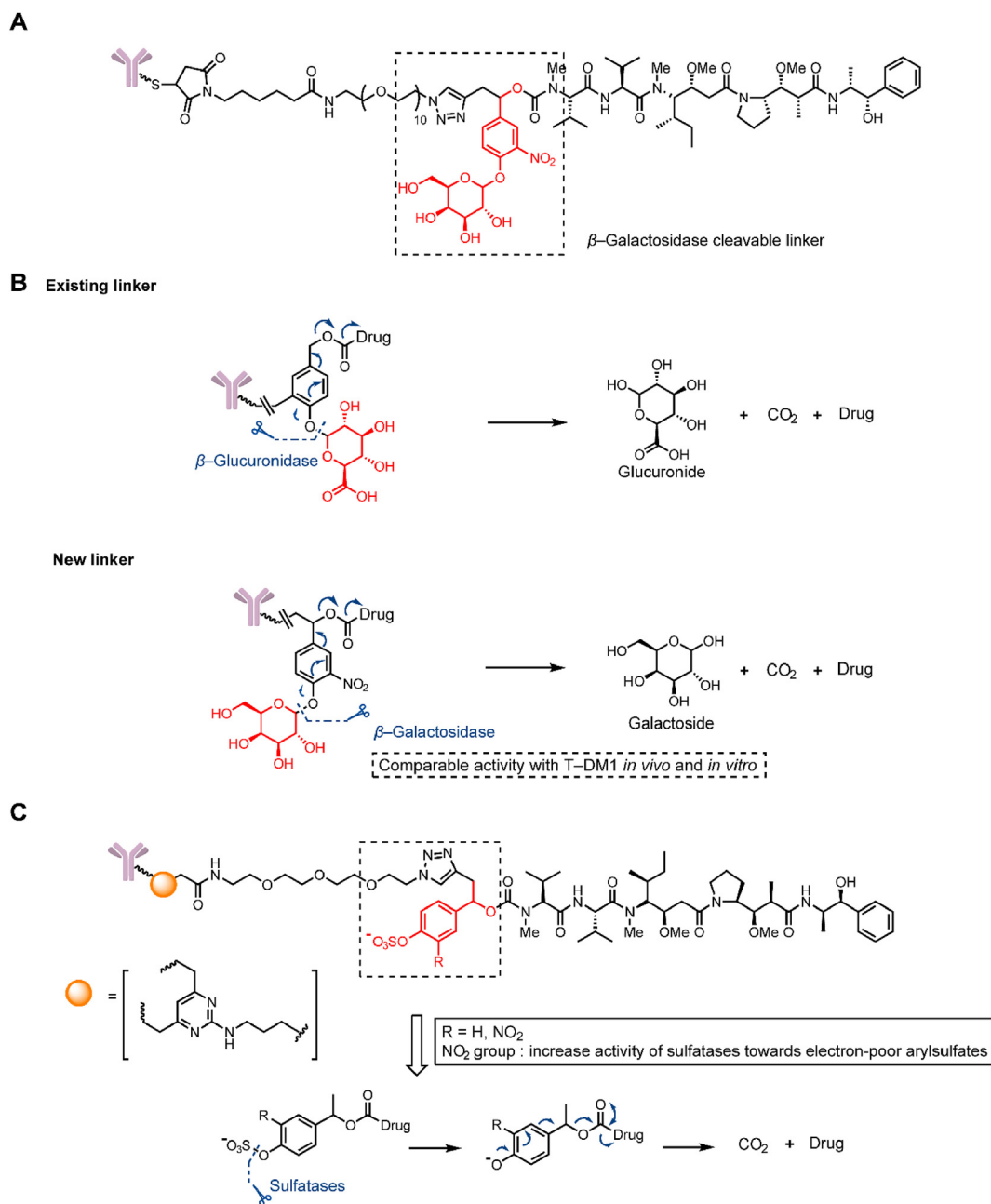


Figure 6 Structures of glycosidase- and sulfatase-cleavable triggers. (A) The structure of a β -glucuronidase-cleavable, linker-containing ADC. Adapted with modification from Ref. 36 © 2017 Elsevier. (B) Release mechanism of β -glucuronidase and β -glucuronidase-cleavable linker-containing ADCs. (C) The structure and release mechanism of sulfatase-cleavable linker-containing ADCs. Adapted with modification from Ref. 37 © 2020 The Royal Society of Chemistry.

that the phosphate/pyrophosphate structure had the potential to be a novel linker. In the same year, Kern et al.¹⁸ replaced the traditional Val-Cit-PAB linker with a phosphate diester structure and synthesized a series of linkers based on the structure of monophosphate, pyrophosphate and triphosphate diesters (Fig. 7B). Compared with the previous linker, the pyrophosphate linker showed extremely high stability over 7 days in mouse and human plasma stabilization experiments. Moreover, the high hydrophilicity of the linker was retained and was able to mitigate the aggregation potential of the ADC with other lipophilic payloads (the solubility of the pyrophosphate diester linker drug is greater than 5 mg/mL). In an *in vitro*

evaluation, ADCs containing pyrophosphate and triphosphate diester linkers are cleaved much more rapidly than monophosphate diesters. According to the analysis of the metabolites of pyrophosphate diester linkers, the ADCs were first hydrolyzed into a monophosphate-payload metabolite and then rapidly produced a prototype drug. The combination of two enzymes may lead to rapid payload release.

Additionally, the cleavable chemical trigger and payload are connected *via* a self-eliminating leaving group, with the PAB group as the current structure^{39,40}. More recently, our group developed a 7-amino-3-hydroxyethyl-coumarin (7-AHC) group as a potent alternative to PAB, which has been employed in a

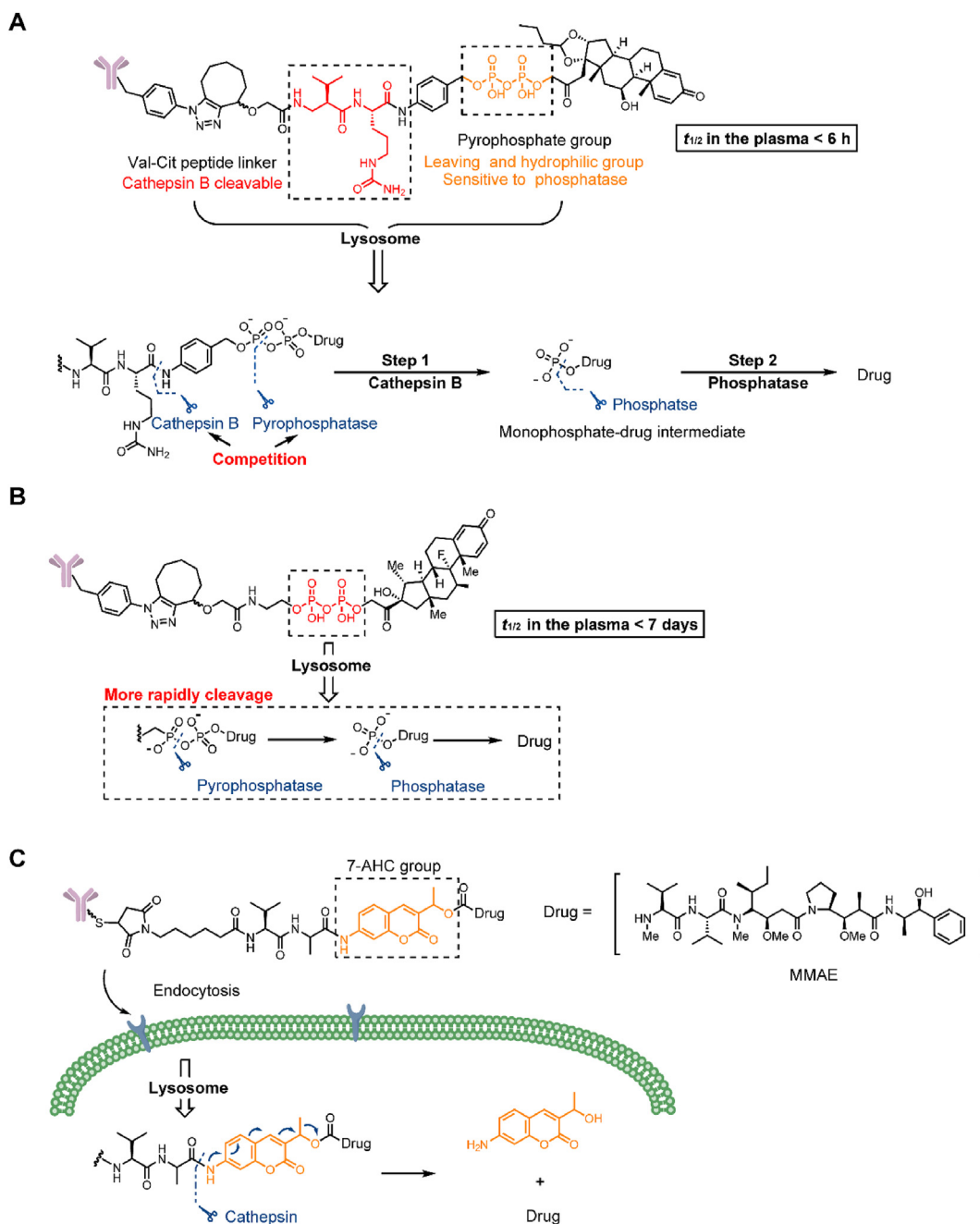


Figure 7 Structures of a pyrophosphate-cleavable trigger and novel leaving group. (A) The structure and release mechanism of Val-Cit-PAB-pyrophosphate linker-containing ADCs. Adapted with modification from Ref. 38 © 2016 American Chemical Society. (B) The structure and release mechanism of pyrophosphate linker-containing ADCs. Adapted with modification from Ref. 39 © 2016 American Chemical Society. (C) The structure and release mechanism of Val-Ala-AHC cleavable linker-containing ADCs. Adapted with modification from Ref. 42 © 2020 Ivyspring International.

dipeptide linker (Fig. 7C)⁴¹. 7-AHC, as a bifunctional fluorescent group, can allow self-elimination cleavage in the presence of cathepsin B for payload release and fluorophore activation. Rapid payload release was observed within 1 h by the 48-fold enhancement in fluorescence. Importantly, the 7-AHC group retained the traditional advantages of a self-eliminating leaving group. ADCs containing a 7-AHC-based dipeptide linker exhibited good stability ($t_{1/2} > 7$ days) and high activity *in vitro* ($IC_{50} = 0.09\text{--}3.74$ nmol/L). In a classic breast cancer model, an

ADC containing the novel linker induced tumor regression at a dose of 1.5 mg/kg and exhibited antitumor efficacy equivalent to that of the marketed Kadcyla.

2.6. Photo-responsive cleavable triggers

The strategy of payload release based on photo-responsive cleavable triggers has gradually emerged in recent years^{42–45}. Photo-responsive cleavable triggers have the following

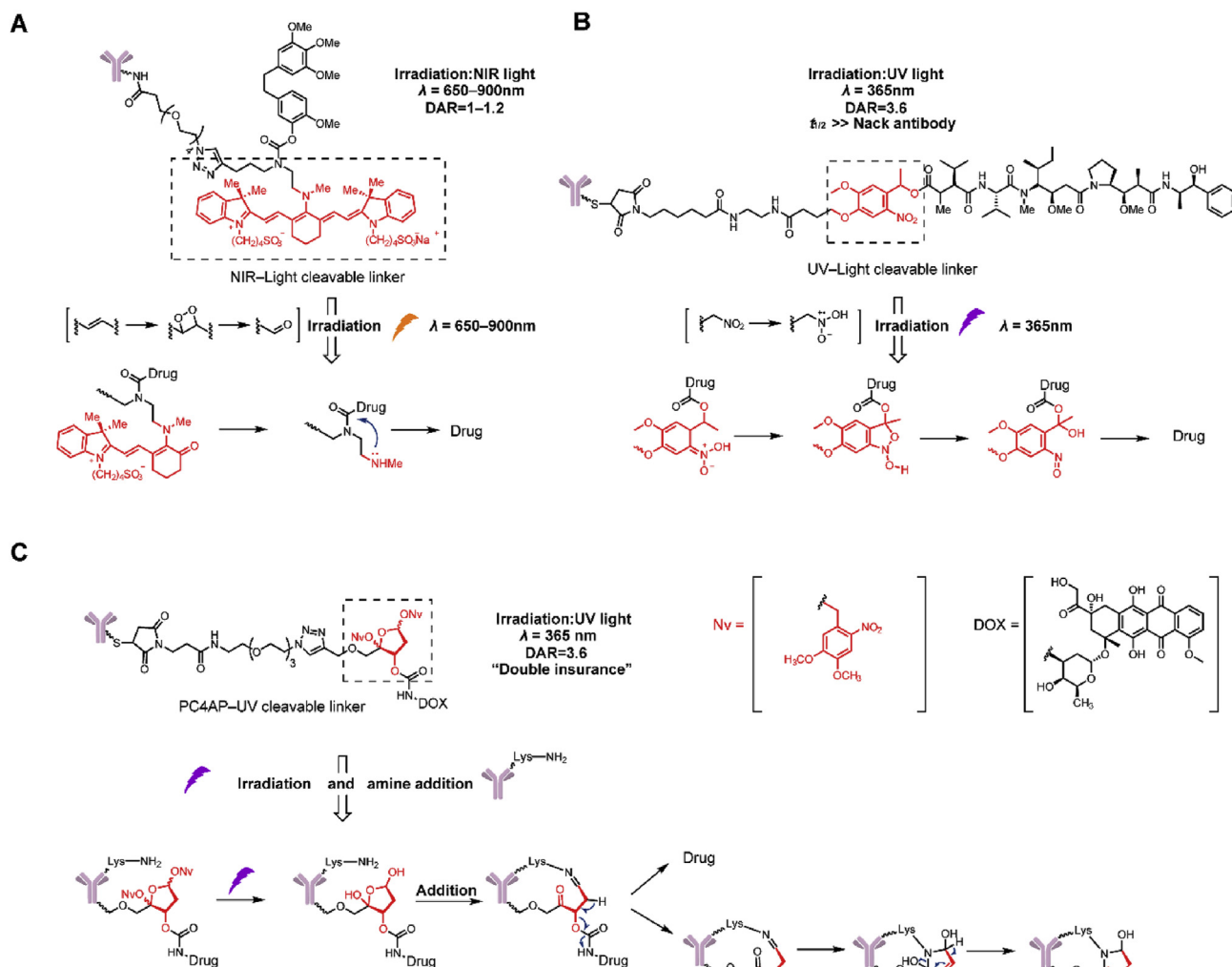


Figure 8 Structures of photo-responsive cleavable triggers. (A) The structure and release of NIR-cleavable linker-containing ADCs. Adapted with modification from Ref. 47 © 2015 WILEY. (B) The structure and release mechanism of UV-cleavable linker-containing ADCs. Adapted with modification from Ref. 48 © 2020 Elsevier. (C) The structure and release mechanism of PC4AP-UV cleavable linker-containing ADCs. Adapted with modification from Ref. 49 © 2019 The Royal Society of Chemistry.

advantages: (1) controlled drug release and effective reduction in off-target toxicity and (2) determination of the cleavage mechanism and no limitation on the intracellular release. Photo-responsive cleavable triggers enjoy the following advantages, including low toxicity, a rapid response, and high sensitivity and specificity.

In 2015, Nani et al.⁴⁶ firstly employed a near-infrared (NIR) light photo-caging strategy for ADCs (Fig. 8A). The photo-responsive cleavable trigger was based on a heptamethine cyanine fluorophore scaffold. Upon irradiation with NIR light ($\lambda = 650\text{--}900\text{ nm}$), the ADCs effectively released the small molecule cytotoxin CA-4 in the irradiated tumor areas in a site-specific manner. In a stability study, the linker without NIR light in human plasma at $37\text{ }^{\circ}\text{C}$ led to minimal release of CA-4 (<1%) after 72 h. In an *in vitro* cytotoxicity experiment, ADCs containing the NIR light-cleavable linker exhibited activity ($\text{IC}_{50} = 16\text{ nmol/L}$) equivalent to CA-4 in an EGFR⁺ cell line upon irradiation and low activity ($\text{IC}_{50} = 1.1\text{ }\mu\text{mol/L}$) without irradiation. However, the self-aggregation and photo-unstable characteristics of this linker limit its applications in biological research and further development as a drug.

More recently, our group initially reported a novel ultraviolet (UV) light-controlled ADC (Fig. 8B)⁴⁷. The linkers introduced a UV light-controlled *O*-nitrobenzyl group as a chemical trigger. In stability and release studies, this linker containing MMAE released <1% under natural light over 6 days and showed the rapid release of MMAE that reached the highest plateau within 10 min upon irradiation. In an *in vitro* cytotoxicity experiment, after irradiation with 365 nm (40 W) UV light, the activities of the *O*-nitrobenzyl linker-containing ADCs were greatly increased (both $\text{EC}_{50} = 0.04\text{ nmol/L}$), and were 50-fold higher than that of unirradiated ADCs. From *in vivo* imaging experiments, it was observed that the *O*-nitrobenzyl linker-containing ADCs have half-lives almost equal to naked antibodies, maintaining the advantage of a long half-life.

In 2019, Zang et al.⁴⁸ reported a photo-responsive, self-cleaving linker employing a photo-caged C40-oxidized abasic site (PC4AP). Compared with the 2 ADCs mentioned, this linker has “double insurance” within a single chemical trigger by design. Upon irradiation at 365 nm, the hydroxyl group of PC4AP undergoes an intramolecular addition reaction with a nearby amine on its own antibody, and a subsequent elimination reaction leads

to cleavage and payload release (Fig. 8C). In the release study, it was confirmed that payloads can be completely released after incubation for 1 h in the presence of both *N*-terminal amines and light, and could not be released under a single light condition. Furthermore, Mal-PC4AP-doxorubicin (DOX) exhibited no cytotoxicity under light conditions in the SK-BR-3 cell line, which coincided with the results of the release study. The peptide-PC4AP-DOX-containing ADC showed toxicity equivalent to the payload DOX in positive cells and no cytotoxicity without irradiation.

Near infrared light ($\lambda = 650\text{--}900\text{ nm}$)-controlled cleavage of ADCs faces the problems of complex structure, self-aggregation, photo-instability, and unfavorable pharmacokinetics *in vivo*^{49,50}. For UV ($\lambda = 365\text{ nm}$)-controlled ADCs, a high dosage of UV is toxic and can lead to oxidative stress, photoaging and immunosuppression^{51,52}. Moreover, UV blue light cannot penetrate patient skin to reach deeply into the tumor area. Only depths of about 100 μm can be reached^{51,52}.

2.7. Bioorthogonal cleavable triggers

Bioorthogonal chemistry refers to a chemical reaction that can occur in the body without interfering with normal biological processes, featuring high selectivity, fast and simple processing and nontoxic byproducts. Therefore, bioorthogonal cleavage pairs are suitable as cleavable triggers^{53,54}. In 2019, Wang et al.⁵⁵ developed a bioorthogonal cleavable linker that employed the classical bioorthogonal cleavage pairs, Cu(I)-2-[4-[[bis[(1-*tert*-butyl)triazol-4-yl)methyl]amino]methyl]triazol-1-yl]acetic acid (BTAA) and dual-substituted propargyloxycarbonyl (dsProc). The bioorthogonal cleavable trigger-containing ADCs release payloads at the cancer cell surface (Fig. 9). Although free copper ions are widely distributed, it has been confirmed that dsProc has high selectivity and cleavage reactivity only to Cu(I)-BTAA. In the *in vitro* toxicity experiments, it was shown that the addition of 50 $\mu\text{mol/L}$ Cu(I)-BTAA decreased the IC_{50} of DOX-dsProc-containing ADCs by 120-fold. While these linkers expanded the cleavage mechanism, they may not be an optimal linker for payloads with poor membrane permeability due to extracellular release.

The study of bioorthogonal-cleavage triggers developed recently and has focused on *in vitro* exploration. Problems remain regarding reaction efficiency, reaction rate, substrate stability, biocompatibility and operation convenience. At present, they cannot be applied *in vivo*, and are far from clinical application.

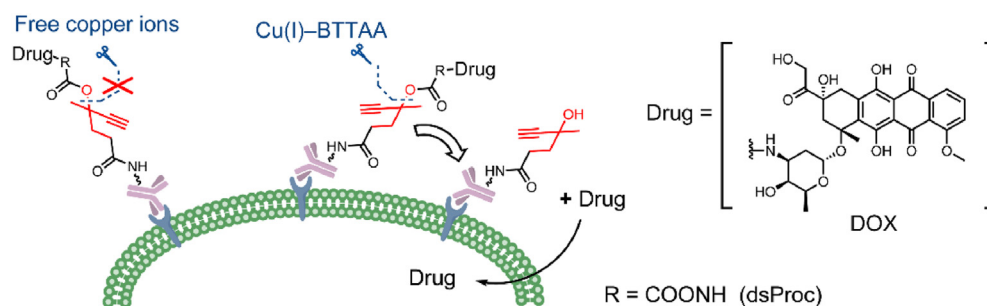


Figure 9 The structures and release mechanism of bioorthogonal-cleavable linker-containing ADCs. Adapted with modification from Ref. 56 © 2019 American Chemical Society.

2.8. Novel noncleavable linkers

Differing from cleavable linkers, noncleavable linkers have no structural chemical trigger for payload release. Therefore, the active part of a noncleavable ADC is comprised of an amino acid appendage, a linker and a cytotoxic payload⁵⁶. A fundamental requirement for noncleavable linkers is that they can not reduce the activity of the payload.

SMCC is a classic noncleavable linker that has been employed in Kadcyla. However, SMCC-based conjugates are still limited due to their instability in the circulatory system and hydrophobic properties¹². In 2016, Igor Dovgan et al.¹⁴ presented 2-(malimidomethyl)-1,3-dioxane (MD) as a potent alternative to the classical SMCC linker (Fig. 10A). Replacing the cyclohexane ring with 1,3-dioxane, the two intracyclic oxygen atoms increased the hydrophilicity of the novel noncleavable linker. Despite the presence of an acetal moiety, the MD-based linker was remarkably stable even at $\text{pH} = 0$. In a human plasma stability study, MD-linker fluorescence conjugates exhibited four times lower fluorescence than the SMCC linker fluorescence conjugates at 72 h. Different from the SMCC linker, the succinimidy ring in the MD linkers underwent fast self-stabilization by ring-opening hydrolysis to avoid a retro-Michael reaction. In another stability study, the MD linker-containing ADCs showed only 3% degradation in 120 h compared to 38% degradation of the same SMCC-containing ADCs. Subsequently, Tobaldi et al.⁵⁷ further explored this novel strategy. By changing the size of the acetal ring and the length of the carbon chain between the acetal and succinimidy moieties, it was proven that increasing the size of the acetal ring and the length of the carbon chain exhibited better succinimidy ring-opening kinetics. In general, the length of the carbon chain was the major determinant for achieving self-stabilization.

In 2017, Gregson et al.⁵⁸ demonstrated three highly hydrophilic noncleavable linkers synthesized by iodoaryl intermediates to connect pyrrolobenzodiazepine (PBD) dimers (Fig. 10B). This noncleavable linker was constructed with hydrophilic PEG chains including an alkyne, a triazole and a piperazine coupled to the PBD dimer through aryl groups. In contrast to the other two linkers, ADCs containing a triazole were completely inactive in the HER2/3⁺ KPL-4 cell line *in vitro*. Equivalent results were also reflected in the *in vivo* experiment. ADCs containing an alkyne and a piperazine achieved tumor suppression in the WSUDLCL2 lymphoma xenograft model at similar doses (0.31 and 1 mg/kg, respectively), while ADCs containing a triazole needed a dose of 36 mg/kg. Interestingly, these linkers were only distinguishable by the three slightly different functional groups, but their activity was

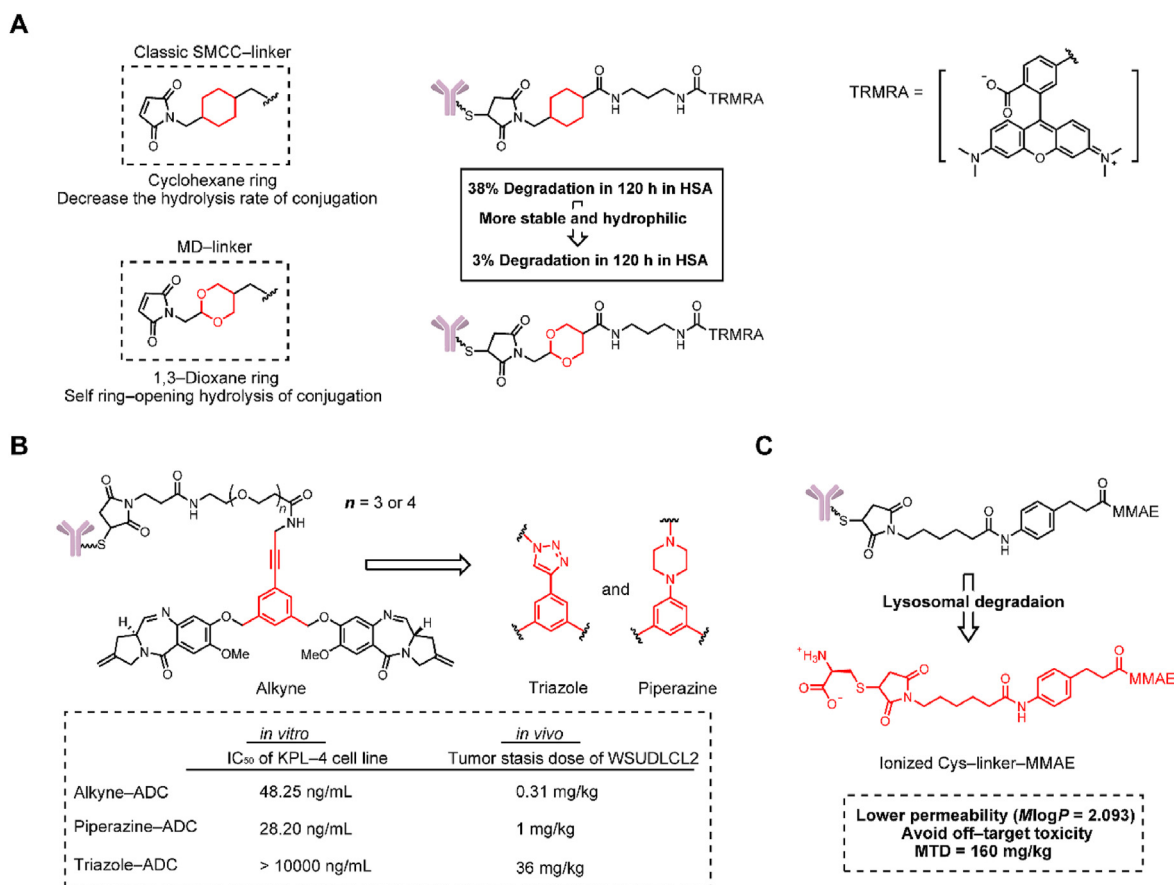


Figure 10 Structures of non-cleavable linkers. (A) The structure of MD non-cleavable linker-containing ADCs. Adapted with modification from Ref. 14 © 2016 Nature Publishing Group. (B) The structure of noncleavable ADCs containing an alkyne, a triazole and a piperazine group, respectively. Adapted with modification from Ref. 59 © 2017 American Chemical Society. (C) The structure of noncleavable linker-MMAE-containing ADCs. Adapted with modification from Ref. 60 © 2020 Multidisciplinary Digital Publishing Institute.

very different. This research suggested that PEG linkers containing alkynes or piperazine would be noncleavable linkers with potential applications.

Without bystander effects, an advantage of the noncleavable linkers is to lower off-target toxicity in normal tissues. Based on this, our group developed a noncleavable ADC with MMAE as the payload, which could broaden the therapeutic window of MMAE-based ADCs (Fig. 10C)⁵⁹. The active part of the noncleavable ADC (L-cysteine (Cys)-linker-MMAE) not only exhibited similar cytotoxicity to that of MMAE (IC₅₀: 10⁻¹¹ mol/L), but also reduced toxicity in the bystander effect test. We thought that the low permeability ($MlogP = 2.093$) helped to avoid off-target toxicity. In the xenograft mouse model, the noncleavable ADC showed significant antitumor activity at a dose of 2.5 mg/kg with a MTD reaching 160 mg/kg, which is almost twofold that of the Val-Ala linker containing ADC.

3. Linker–antibody attachments of the linker

Linker–antibody attachments act as a bridge connecting the linker and antibody. At present, two main challenges remain for the linker–antibody attachment. The first one is the retro-Michael elimination of the classical maleimide attachment, which can eventually lead to off-target toxicity. The optimization in the chemical structures over the last 5 years are reviewed here. The

second challenge is the heterogeneous DAR values. Essentially, the approved ADCs are mixtures of different DAR values. Developing a homogeneous ADC has always been the goal. Currently there are 2 strategies: site-specific conjugation technology and chemical structural modification of the linker–antibody attachment. Site-specific conjugation through antibody engineering is extensively reviewed elsewhere^{60–62}.

3.1. Maleimide attachment

Maleimide structure conjugation has been widely used in ADCs and exhibits the inherent advantages of fast reaction kinetics and excellent thiol specificity. However, thiol-maleimide coupling is susceptible to retro-Michael reaction, which leads to the instability of ADCs in the circulatory system and eventually a low therapeutic index⁶³.

As early as 2014, Lyon et al.⁶⁴ found that the problem of retro-Michael elimination could be chemically solved by the self-hydrolysis of thiosuccinimide. In 2015, Christie et al.⁶⁵ and Fontaine et al.⁶⁶ developed several modified functional groups attached to the maleimide ring to stabilize cysteine conjugation, such as proximal amines and electron-withdrawing groups (Fig. 11A). But we think the real breakthrough work might belong to Christie et al.⁶⁷ In 2017, their group described a *N*-phenyl maleimide attachment containing linkers (noncleavable and Val-

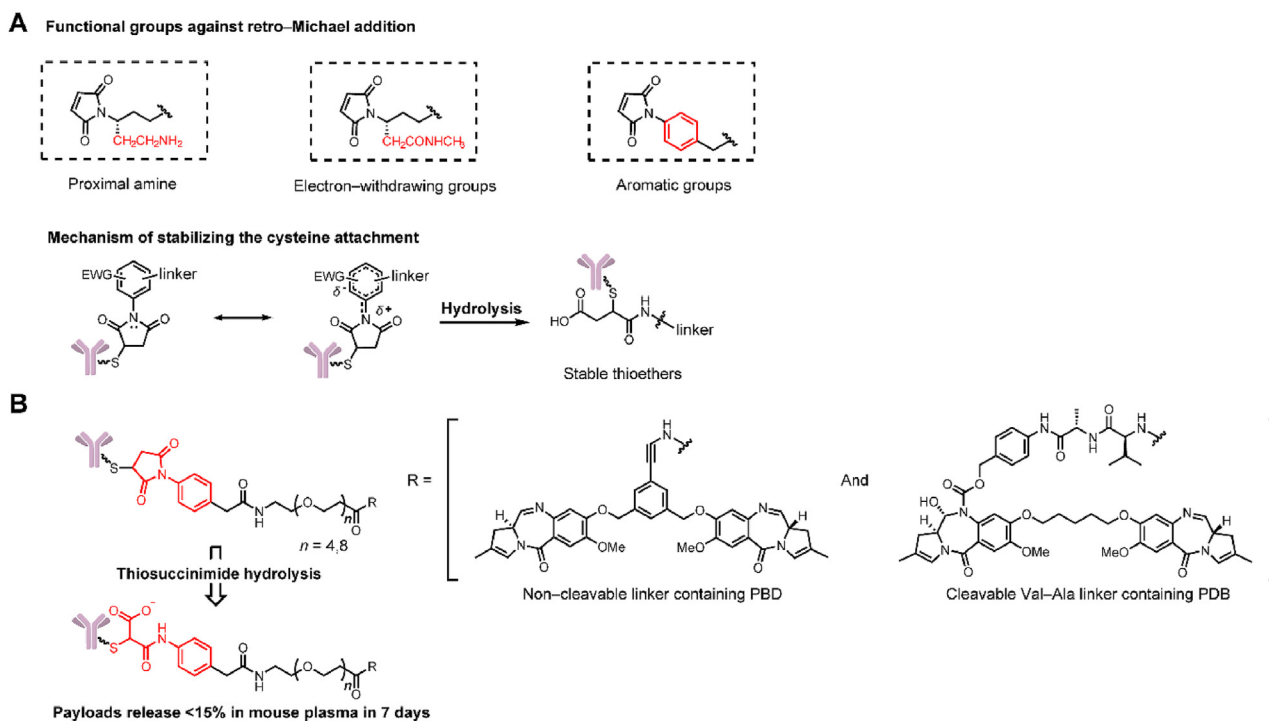


Figure 11 Structures of the optimized maleimide attachment. (A) The structure and mechanism of optimized maleimide attachment by proximal amines and electron-withdrawing groups. (B) The structure and mechanism of optimized maleimide attachment by *N*-phenyl maleimide. Adapted with modification from Ref. 68 © 2017 Multidisciplinary Digital Publishing Institute.

Ala linkers, Fig. 11B), which could stabilize thiol conjugation through rapid thiosuccinimide hydrolysis. Compared with *N*-alkyl maleimide attachment employing the same linkers, the non-cleavable ADCs containing *N*-phenyl maleimide exhibited higher conjugation stability in mouse plasma over 7 days (payload release 15% vs. 45%). Similarly for the *N*-phenyl maleimide-Val-Cit linker, ADCs containing *N*-phenyl maleimide retain over 90% conjugation. In contrast, ADCs containing *N*-alkyl maleimide retain only 65% conjugation. *N*-phenyl maleimide-containing ADCs exhibited toxicities equivalent to those of *N*-alkyl ADCs in antigen positive cell lines in *in vitro* cytotoxicity analysis. In the xenograft mouse model, ADCs containing a noncleavable linker with *N*-phenyl maleimide attachment had better antitumor activity *in vivo* than ADCs containing *N*-alkyl maleimide. The former arrested tumor growth at a dose of 1 mg/kg, while the latter exhibited no antitumor activity at the same dose⁶⁷.

3.2. Bis(vinylsulfonyl)piperazine attachment

As early as 2006, Shaunak et al.⁶⁸ developed a 3-carbon bridge through bisulfones to cross-link two cysteine residues. Subsequently in 2014, Badescu et al.⁶⁹ successfully applied this attachment to design and synthesize a homogeneous and stable ADC with a DAR = 4. However, this method commonly led to the production of half-antibodies by conjugation in hinge regions of the monoclonal antibody (Fig. 12A). In 2020, Huang et al.⁷⁰ continued to develop a novel bis(vinylsulfonyl)piperazine (BVP) linker for the selective conjugation of disulfides mostly in the Fab regions (Fig. 12A). Compared with previous work, this structure could efficiently avoid the formation of a half-antibody⁷¹ and facilitate the construction of highly homogeneous ADCs with a

DAR = 2. In a stability experiment the BVP conjugates maintained high stability without a decrease in DAR after 7 days at 37 °C in human plasma. In an *in vitro* cytotoxicity study, a BVP attachment-containing ADC in HER2 negative MDA-MB-231 cells exhibited far lower toxicity than Kadcyla (>500 vs. 51.5 ± 15.7 nmol/L), and these differences in toxicity in antigen-negative cells suggested that the ADC containing BVP conjugation had a lower off-target toxicity.

3.3. *N*-methyl-*N*-phenylvinylsulfonamide attachment

In addition to modifying the existing maleimide conjugation, Huang et al.⁷² introduced *N*-methyl-*N*-phenylvinylsulfonamide for cysteine-selective conjugation to prevent the retro-Michael reaction (Fig. 12B). *N*-Methyl-*N*-phenylvinylsulfonamide conjugation exhibited high stability after 72 h in the presence of the thiol nucleophile glutathione. ADCs containing this conjugation could be defined as a DAR = 8.

3.4. Pt(II)-based attachment

Waalboer et al.⁷³ first proposed the conjugation of histidine onto trastuzumab with platinum(II) in 2015 and explored the preliminary stability of platinum(II) conjugates. Subsequently, in 2016, Sijbrandi et al.⁷⁴ developed a metal-organic [ethylenediamine platinum(II)]²⁺ linker, termed Lx®, and further constructed trastuzumab-Lx-desferoxamine (DFO)/monomethyl auristatin F (MMAF) ADCs (Fig. 12C). Because histidine is ubiquitous in antibodies and the simple two-step operation, Lx® conjugation has versatile applicability in ADCs. The advantages of this type of conjugation are mainly exhibited in good manufacturability and

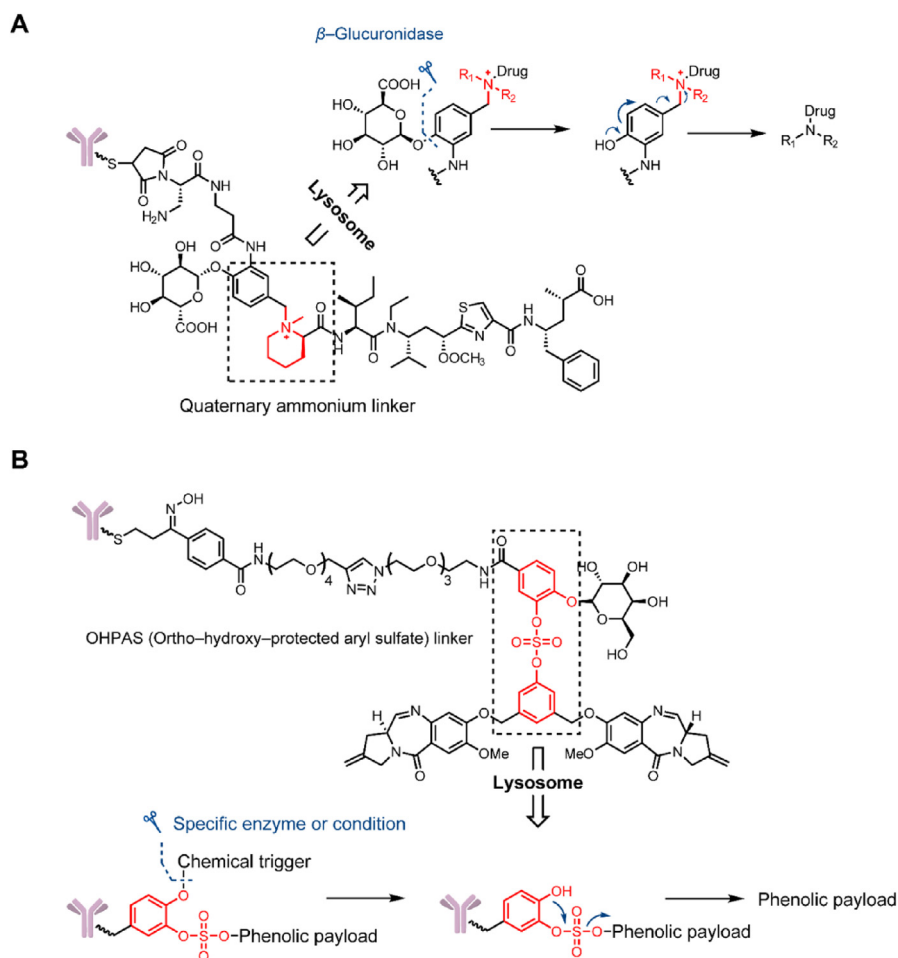


Figure 13 Structures of novel linker–payload attachments. (A) Structures of tertiary amine attachments. Adapted with modification from Ref. 79 © 2016 American Association for Cancer Research. (B) Structures of OHPAS attachments. Adapted with modification from Ref. 83 © 2019 American Chemical Society.

stability studies, the linker employing a chemical trigger of β -galactoside showed stability for 7 days in both PBS and plasma. To further confirm the versatile applications of the OHPAS attachment-containing linker, the researchers synthesized β -galactoside-OHPAS attachment-containing ADCs loaded with 8 payloads, and these ADCs were tested for their activity *in vitro*. The ADCs exhibited IC_{50} values that were equivalent to or even higher than that of Kadcyra in antigen-positive cell lines. Similar results were also observed in *in vivo* studies; in the amanitin-containing ADC treatment group, the tumor completely resolved from Day 10 to Day 60 after administration (2 and 0.5 mg/kg). In addition to containing different payloads, researchers have tried to employ multiple triggering parts, such as β -galactosidase, β -glucuronide, and levulinic esters, in OHPAS linkers to identify the practical value of this attachment.

5. Absorption, distribution, metabolism, and excretion (ADME) optimization of the linker

With the development of ADCs, hydrophilicity must be considered⁸³. Low hydrophilicity of the linker shows the following disadvantages: (1) low conjugate efficiency and DAR, (2) polymerization and sedimentation in human plasma, (3) off-target toxicity by nonspecific uptake, and (4) undesirable

pharmacokinetics by rapid elimination from plasma^{84,85}. Therefore, the hydrophilicity of ADCs is crucial. Currently, strategies for improving the hydrophilicity of ADCs are mainly divided into two categories: (1) incorporating PEG or sulfonate moieties into the linker of the ADC^{86–89}; or (2) developing highly hydrophilic linkers, such as phosphate-based linkers or charged linkers like [ethylene diamine platinum III]²⁺ linkers mentioned at the beginning of this review. In addition to linker hydrophilicity affecting the plasma kinetics and off-target toxicity of ADCs, a series of studies by Zhang et al. showed that linkers will also affect payload kinetics in tumors, and thereby determine the *in vivo* efficacy of ADCs.

5.1. Hydrophilicity optimization

There have been many studies on strategies to increase hydrophilicity with PEG, and studies on the relationship between hydrophilicity and the off-target effects of ADCs have also been conducted in recent years. In 2020, Simmons et al.⁹⁰ described a family of MMAE-based ADCs with linkers containing PEG chains of 0, 4, 8 or 12 units. To investigate the relationship between off-target toxicity and hydrophilicity, the ADCs in this study were linked with nontargeted antibodies. In the tolerance experiments, all mice died in the PEG0 ADC group on the 5th day

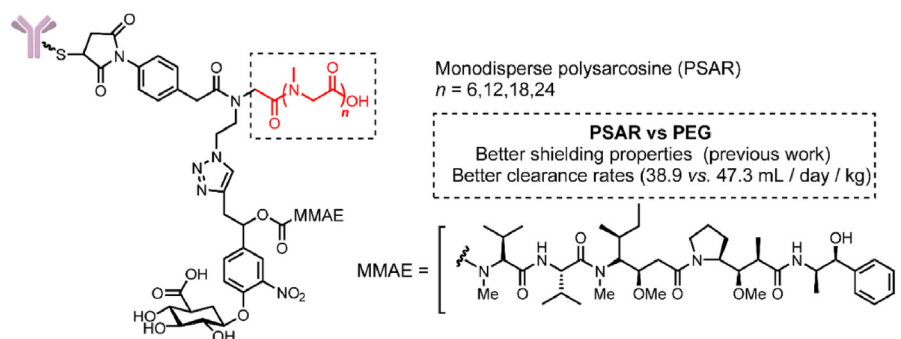


Figure 14 The structure of PSAR- β -glucuronidase cleavable linker-containing ADCs. Adapted with modification from Ref. 92 © 2019 Royal Society of Chemistry.

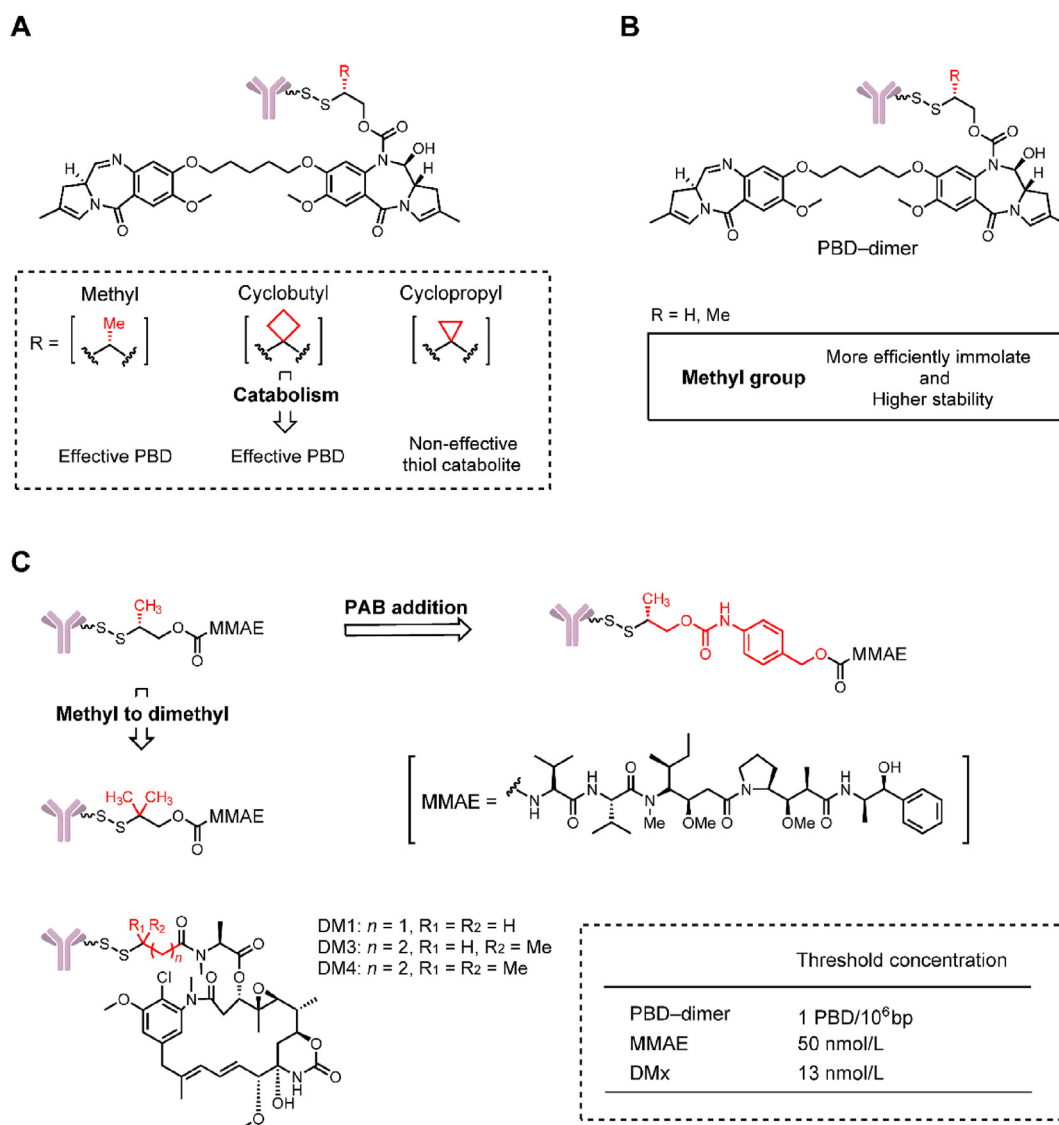


Figure 15 Effects on payload kinetics in tumors of linkers. (A) The structure of PBD-dimer-containing ADCs. Adapted with modification from Ref. 93 © 2016 American Society for Pharmacology and Experimental Therapeutics. (B) The structure and *in vivo* evaluation of PBD-dimer-containing ADCs. Adapted with modification from Ref. 94 © 2018 American Association for Cancer Research. (C) The structural optimization of MMAE-containing ADCs and the structure of DMx-containing ADCs. Adapted with modification from Ref. 95 © 2019 American Society for Pharmacology and Experimental Therapeutics.

at the 20 mg/kg dose, but the survival rate of the PEG8 and PEG12 groups was 100% after 28 days. After immunohistochemical (IHC) staining of the mouse livers, PEG0-containing ADCs showed nonspecific uptake and released a large quantity of MMAE after 2 h at a dose of 10 mg/kg. It was therefore proven that the low dose tolerance of ADCs with low hydrophilicity was caused by nonspecific liver absorption. Meanwhile the ADCs containing PEG12 showed slower plasma clearance (7.3 mL·kg/day) and longer plasma exposure than those containing PEG0 (>46.3 mL·kg/day). In summary, ADCs with relatively high hydrophilicity could improve the pharmacokinetic parameters of ADCs, and significantly decrease the nonspecific uptake and off-target toxicity.

In addition to incorporating short PEG chains into the linker, numerous hydrophilic fragments have been tested to improve linker properties. In 2019, Viricel et al.⁹¹ developed monodisperse polysarcosine (PSAR) as a hydrophobic masking entity to construct highly loaded (DAR = 8) β -glucuronidase-responsive ADCs (Fig. 14). PSAR is a polypeptide composed of endogenous sarcosine amino acids that is employed as a hydrophilic block. In previous work, it was confirmed that PSAR provides slightly better shielding properties than PEG at equal lengths. In this pharmacokinetic study, PSAR more efficiently reduced clearance rates than PEG (38.9 vs. 47.3 mL/day/kg). In a xenograft mouse model, a single dose of the ADC containing PSAR12 at 3 mg/kg induced complete tumor regression. At the same dose, Kadcyla was only able to promote tumor growth delay.

5.2. Payload kinetics in tumors

In 2016, Zhang et al.⁹² found that anti-CD22 disulfide-PBD-ADC containing methyl- and cyclobutyl-substituted disulfide linkers exhibited strong efficacy in a WSU-DLCL2 xenograft mouse model, whereas an ADC with a cyclopropyl linker was inactive (Fig. 15A). This finding was very interesting because the cyclobutyl and cyclopropyl substitutions lead to a large difference in the efficacy of ADCs. Further *in vivo* pharmacokinetic studies showed that cyclobutyl-containing ADCs could effectively deliver the PBD dimer (1.0–2.0 nmol/L) in tumors at both 24 and 96 h after dosing. In contrast, cyclopropyl-containing ADC could only release the ineffective cyclopropyl thiol catabolite in tumor (4.3–7.5 nmol/L). In 2018, they carried out a further research on the methyl-substituted disulfide linker (Fig. 15B)⁹³. Results suggested that the methyl-containing linker self-cleaved much more efficiently and exhibited higher stability than the non-methyl-containing linker. Payload release in tumor is a net result of disulfide cleavage and subsequent self-cleavage.

In 2019, the delivery of other commonly used payloads, such as maytansinoids (*e.g.*, DMx), auristatins (*e.g.*, MMAE) by different linkers was studied (Fig. 15C)⁹⁴. This study further verified that intratumoral payload exposures directly related to the structure of linker. Similar to PBD, MMAE could also be conjugated to the antibody through a self-cleavage disulfide linker. The double-methyl-disulfide (DiMe-SS)-MMAE-ADC showed higher tumor delivery (42.1 vs. 19.1 nmol/L) and tumor growth inhibition (69% vs. 50%) than the methyl-disulfide (Me-SS)-MMAE-ADC. Addition of PAB group to the Me-SS-MMAE-ADC could further improve the MMAE delivery (87.1 nmol/L) in tumor, giving a corresponding 30% tumor regression. The maytansinoids could be directly conjugated to the THIOMAB antibody through the disulfide bond. Direct conjugation of DM4 to light chain at K149C resulted in a very stable ADC with no DAR loss at day 10 *in vivo*.

Their studies also suggested a threshold concentration and a plateau effect for an ADC. A threshold concentration of intratumor payload was required to support sustained efficacy, which was approximately 1 PBD/10⁶ bp for PBD-ADCs and 50 nmol/L for MMAE-ADCs, and 13 nmol/L for DMx-ADCs. A plateau effect means that an ADC can deliver an excessive level of payload to tumors that does not enhance efficacy.

6. Conclusions

There are numerous developments on the structural optimization and mechanism expansion of ADCs over the past five years. Firstly, and most importantly, novel chemical triggers have been developed to obtain higher selectivity in delivery to tumors. For instance, the cBu trigger, the silyl ether trigger, the TRX trigger are valuable approaches. Particularly, novel photo-responsive cleavable triggers and bioorthogonal cleavable triggers could break the intracellular drug release restrictions for traditional ADCs, and provide an opportunity for the use of nonendocytic antibodies, but might not work for low membrane permeability payloads, such as MMAE. Secondly, for linker-antibody attachment, there are two main problems that remain to be solved. The first problem is the retro-Michael elimination of the classical maleimide attachment. Fortunately, *N*-phenyl maleimide attachment could significantly improve the stability of ADCs with minor structural alterations, with promising prospects. The second problem is the heterogeneity of the DAR values. Although site-specific conjugation could solve this problem by modifying the antibodies, developing new linker-antibody attachments might be another effective way. For instance, the BVP attachment could help to produce highly homogeneous ADCs with a DAR = 2. Thirdly, the linker plays an important role in the pharmacokinetics of ADCs. It can not only affect the plasma kinetics by adding hydrophilic fragments, but also affect the kinetics of payload release in tumors by structural optimization. Finally, with the rapid expansion of the payload arsenal, more and more linker-payload attachments have been developed in recent years. In particular, the quaternary ammonium attachment could connect all payloads with a tertiary amine, such as Carfilzomib, Vinblastine, Duocarmycin, Rifabutin, etc. In conclusion, additional studies are needed to confirm the real effects of the novel linkers, despite their encouraging initial data.

7. Challenges and outlook

An ADC is a precise drug delivery system formed by the combination of a highly targeted antibody, a well-designed linker and a highly active payload. The complex composition of ADCs leads to following challenges at present: (1) toxicity problems remain to be solved. Although ADCs have greatly improved the targeting efficiency (over 100-fold⁹⁵) compared to traditional chemotherapeutics, research has shown that less than 1% of the dosed ADCs accumulate in the tumors⁹⁶. The danger is that the payloads, commonly 100-fold more toxic than conventional chemotherapeutic drugs, could be non-specifically released in normal tissues by the linkers. This eventually leads to systemic adverse effects and low MTD of ADCs. For instance, the MTD of Adcetris and Kadcyla is only 1.8 and 3.6 mg/kg respectively^{97,98}. The limited MTD greatly limits the therapeutic potential of ADCs. In the future, more selective linkers can not only release payload rapidly in tumor tissues, but also effectively reduce the off-target toxicity in normal tissues.

This important scientific assumption is the guide for our present work, and our unpublished data have initially supported this idea. (2) Drug resistance is another challenge of ADCs. Although the mechanisms of drug resistance for ADCs have not been determined, research has shown that down-regulation of target antigen, reduction of internalization of ADCs and efflux of the active payload are possible causes. For instance, the classic payloads, such as MMAE and DM1, are easily transported by adenosine triphosphate (ATP) binding proteins and lead to drug resistance. Therefore, SN-38, PBD and other novel payloads have been employed in ADCs, such as the Trodelvy. The discovery of new payloads requires the development of new linkers. (3) Full-length antibodies employed in ADCs inevitably face the problem of limited penetration of solid tumors and limited endocytotic efficiency. Along with employing smaller nano-antibodies to improve efficiency, this limitation may also be solved by using linkers with extracellular release capacity. Our group has made an initial attempt to design and synthesize photo-responsive linkers for extracellular release, but the reliability and validity needs further *in vivo* studies. (4) The relatively complex structure of linkers leads to difficulties in preclinical studies and in clinical applications. Therefore, the development of linkers with simplified structures and integrated functions may be another research direction. Our group attempted to integrate therapy and imaging in a theranostic ADC, which would help promote the pre-clinical study of ADCs. Thomas et al.³⁰ simplified the linker by directly connecting the payloads to the antibody through a disulfide bond. We believe that with the development of antibody technology, linker technology and novel payloads, ideal ADCs with disruptive efficacy will be finally developed to promote the development of personalized medicines.

Acknowledgments

This work was funded by the Chinese National Natural Science Foundation (Grant Nos. 81872736 and 81903451), and the China Postdoctoral Science Foundation (Grant No. 2019M664015).

Author contributions

Zheng Su and Dian Xiao contributed equally to this work. Zheng Su and Dian Xiao: writing – review & editing, data curation. Fei Xie, Lianqi Liu and Yanming Wang: investigation, data curation, validation. Shiyong Fan, Xinbo Zhou and Song Li: conceptualization, project administration, funding acquisition.

Conflicts of interest

The authors have no conflicts of interest to declare.

References

1. Strebhardt K, Ullrich A. Paul Ehrlich's magic bullet concept: 100 years of progress. *Nat Rev Cancer* 2008;**8**:473–80.
2. Lamb YN. Inotuzumab ozogamicin: first global approval. *Drugs* 2017;**77**:1603–10.
3. Dhillon S. Moxetumomab pasudotox: first global approval. *Drugs* 2018;**78**:1763–7.
4. Deeks ED. Correction to: polatuzumab vedotin: first global approval. *Drugs* 2019;**79**:1829.
5. Chang E, Weinstock C, Zhang L, Charlab R, Dorff SE, Gong Y, et al. FDA approval summary: enfortumab vedotin for locally advanced or metastatic urothelial carcinoma. *Clin Cancer Res* 2020;**27**:922–7.
6. Greenblatt K, Khaddour K. Trastuzumab. StatPearls Publishing LLC; Dec 19, 2020. Available from: <https://www.ncbi.nlm.nih.gov/books/NBK532246/>.
7. Markham A. Belantamab mafodotin: first approval. *Drugs* 2020;**80**:1607–13.
8. Wahby S, Fashoyin-Aje L, Osgood CL, Cheng J, Fiero MH, Zhang L, et al. FDA approval summary: accelerated approval of sacituzumab govitecan-hziy for third line treatment of metastatic triple-negative breast cancer (mTNBC). *Clin Cancer Res* 2021;**27**:1850–4.
9. Lyon R. Drawing lessons from the clinical development of antibody–drug conjugates. *Drug Discov Today Technol* 2018;**30**:105–9.
10. Hamann PR, Hinman LM, Hollander I, Beyer CF, Lindh D, Holcomb R, et al. Gemtuzumab ozogamicin, a potent and selective anti-CD33 antibody-calicheamicin conjugate for treatment of acute myeloid leukemia. *Bioconjug Chem* 2002;**13**:47–58.
11. Perini GF, Pro B. Brentuximab vedotin in CD30⁺ lymphomas. *Biol Ther* 2013;**3**:15–23.
12. Lambert JM, Chari RV. Ado-trastuzumab emtansine (T-DM1): an antibody–drug conjugate (ADC) for HER2⁺ positive breast cancer. *J Med Chem* 2014;**57**:6949–64.
13. Othus M, Appelbaum FR, Petersdorf SH, Kopecky KJ, Slovak M, Nevill T, et al. Fate of patients with newly diagnosed acute myeloid leukemia who fail primary induction therapy. *Biol Blood Marrow Transplant* 2015;**21**:559–64.
14. Dogan I, Kolodych S, Koniev O, Wagner A. 2-(Maleimidomethyl)-1,3-dioxanes (MD): a serum-stable self-hydrolysable hydrophilic alternative to classical maleimide conjugation. *Sci Rep* 2016;**6**:30835.
15. Ponte JF, Sun X, Yoder NC, Fishkin N, Laleau R, Coccia J, et al. Understanding how the stability of the thiol-maleimide linkage impacts the pharmacokinetics of lysine-linked antibody-maytansinoid conjugates. *Bioconjug Chem* 2016;**27**:1588–98.
16. Pillow TH, Tien J, Parsons-Repointe KL, Bhakta S, Li H, Staben LR, et al. Site-specific trastuzumab maytansinoid antibody–drug conjugates with improved therapeutic activity through linker and antibody engineering. *J Med Chem* 2014;**57**:7890–9.
17. Lehar SM, Pillow T, Xu M, Staben L, Kajihara KK, Vandlen R, et al. Novel antibody–antibiotic conjugate eliminates intracellular *S. aureus*. *Nature* 2015;**527**:323–8.
18. Kern JC, Cancilla M, Dooney D, Kwasnjuk K, Zhang R, Beaumont M, et al. Discovery of pyrophosphate diesters as tunable, soluble, and bioorthogonal linkers for site-specific antibody–drug conjugates. *J Am Chem Soc* 2016;**138**:1430–45.
19. Caculitan NG, Dela Cruz Chuh J, Ma Y, Zhang D, Kozak KR, Liu Y, et al. Cathepsin B is dispensable for cellular processing of cathepsin B-cleavable antibody–drug conjugates. *Cancer Res* 2017;**77**:7027–37.
20. Wei B, Gunzner-Toste J, Yao H, Wang T, Wang J, Xu Z, et al. Discovery of peptidomimetic antibody–drug conjugate linkers with enhanced protease specificity. *J Med Chem* 2018;**61**:989–1000.
21. Dorywalska M, Dushin R, Moine L, Farias SE, Zhou D, Navaratnam T, et al. Molecular basis of valine-citrulline-PABC linker instability in site-specific ADCs and its mitigation by linker design. *Mol Cancer Ther* 2016;**15**:958–70.
22. Singh R, Setiady YY, Ponte J, Kovtun YV, Lai KC, Hong EE, et al. A new triglycyl peptide linker for antibody–drug conjugates (ADCs) with improved targeted killing of cancer cells. *Mol Cancer Ther* 2016;**15**:1311–20.
23. Wang Y, Fan S, Zhong W, Zhou X, Li S. Development and properties of valine-alanine based antibody–drug conjugates with monomethyl auristatin E as the potent payload. *Int J Mol Sci* 2017;**18**:1860.
24. Reid EE, Archer KE, Shizuka M, Wilhelm A, Yoder NC, Bai C, et al. Effect of linker stereochemistry on the activity of indolinobenzodiazepine containing antibody–drug conjugates (ADCs). *ACS Med Chem Lett* 2019;**10**:1193–7.
25. Salomon PL, Reid EE, Archer KE, Harris L, Maloney EK, Wilhelm AJ, et al. Optimizing lysosomal activation of antibody–drug conjugates (ADCs) by incorporation of novel cleavable dipeptide linkers. *Mol Pharm* 2019;**16**:4817–25.

26. Casey JR, Grinstein S, Orlowski J. Sensors and regulators of intracellular pH. *Nat Rev Mol Cell Biol* 2010;**11**:50–61.
27. Govindan DV, Cardillo TM, Sharkey RM, Tat F, Gold DV, Goldenberg DM. Milatuzumab-SN-38 conjugates for the treatment of CD74⁺ cancers. *Mol Cancer Ther* 2013;**12**:968–78.
28. Wang Y, Fan S, Xiao D, Xie F, Li W, Zhong W, et al. Novel silyl ether-based acid-cleavable antibody–MMAE conjugates with appropriate stability and efficacy. *Cancers (Basel)* 2019;**11**:957.
29. Mills BJ, Lang CA. Differential distribution of free and bound glutathione and cyst(e)ine in human blood. *Biochem Pharmacol* 1996;**52**:401–6.
30. Pillow TH, Sadowsky JD, Zhang D, Yu SF, Del Rosario G, Xu K, et al. Decoupling stability and release in disulfide bonds with antibody–small molecule conjugates. *Chem Sci* 2017;**8**:366–70.
31. Pillow TH, Schutten M, Yu SF, Ohri R, Sadowsky J, Poon KA, et al. Modulating therapeutic activity and toxicity of pyrrolbenzodiazepine antibody–drug conjugates with self-immolative disulfide linkers. *Mol Cancer Ther* 2017;**16**:871–8.
32. Torti SV, Torti FM. Iron and cancer: more ore to be mined. *Nat Rev Cancer* 2013;**13**:342–55.
33. Spangler B, Fontaine SD, Shi Y, Sambucetti L, Mattis AN, Hann B, et al. A novel tumor-activated prodrug strategy targeting ferrous iron is effective in multiple preclinical cancer models. *J Med Chem* 2016;**59**:11161–70.
34. Spangler B, Kline T, Hanson J, Li X, Zhou S, Wells JA, et al. Toward a ferrous iron-cleavable linker for antibody–drug conjugates. *Mol Pharm* 2018;**15**:2054–9.
35. Jeffrey SC, Andreyka JB, Bernhardt SX, Kissler KM, Kline T, Lenox JS, et al. Development and properties of beta-glucuronide linkers for monoclonal antibody–drug conjugates. *Bioconjug Chem* 2006;**17**:831–40.
36. Kolodych S, Michel C, Delacroix S, Koniev O, Ehkirch A, Eberova J, et al. Development and evaluation of beta-galactosidase-sensitive antibody–drug conjugates. *Eur J Med Chem* 2017;**142**:376–82.
37. Bargh JD, Walsh SJ, Isidro-Llobet A, Omarjee S, Carroll JS, Spring DR. Sulfatase-cleavable linkers for antibody–drug conjugates. *Chem Sci* 2020;**11**:2375–80.
38. Kern JC, Dooney D, Zhang R, Liang L, Brandish PE, Cheng M, et al. Novel phosphate modified cathepsin B linkers: improving aqueous solubility and enhancing payload scope of ADCs. *Bioconjug Chem* 2016;**27**:2081–8.
39. Carl PL, Chakravarty PK, Katzenellenbogen JA. A novel connector linkage applicable in prodrug design. *J Med Chem* 1981;**24**:479–80.
40. Erez R, Shabat D. The azaquinone-methide elimination: comparison study of 1,6- and 1,4-eliminations under physiological conditions. *Org Biomol Chem* 2008;**6**:2669–72.
41. Xiao D, Zhao L, Xie F, Fan S, Liu L, Li W, et al. A bifunctional molecule-based strategy for the development of theranostic antibody–drug conjugate. *Theranostics* 2021;**11**:2550–63.
42. Fodor SP, Read JL, Pirrung MC, Stryer L, Lu AT, Solas D. Light-directed, spatially addressable parallel chemical synthesis. *Science* 1991;**251**:767–73.
43. Pelliccioli AP, Wirz J. Photoremovable protecting groups: reaction mechanisms and applications. *Photochem Photobiol Sci* 2002;**1**:441–58.
44. Bryden F, Maruani A, Rodrigues JMM, Cheng MHY, Savoie H, Beeby A, et al. Assembly of high-potency photosensitizer-antibody conjugates through application of dendron multiplier technology. *Bioconjug Chem* 2018;**29**:176–81.
45. Ito K, Mitsunaga M, Nishimura T, Saruta M, Iwamoto T, Kobayashi H, et al. Near-infrared photochemoimmunotherapy by photoactivatable bifunctional antibody–drug conjugates targeting human epidermal growth factor receptor 2 positive cancer. *Bioconjug Chem* 2017;**28**:1458–69.
46. Nani RR, Gorka AP, Nagaya T, Kobayashi H, Schnermann MJ. Near-IR light-mediated cleavage of antibody–drug conjugates using cyanine photocages. *Angew Chem Int Ed Engl* 2015;**54**:13635–8.
47. Li J, Xiao D, Xie F, Li W, Zhao L, Sun W, et al. Novel antibody–drug conjugate with UV-controlled cleavage mechanism for cytotoxin release. *Bioorg Chem* 2021;**111**:104475.
48. Zang C, Wang H, Li T, Zhang Y, Li J, Shang M, et al. A light-responsive, self-immolative linker for controlled drug delivery via peptide– and protein–drug conjugates. *Chem Sci* 2019;**10**:8973–80.
49. Xu Y, Li Z, Malkovskiy A, Sun S, Pang Y. Aggregation control of squaraines and their use as near-infrared fluorescent sensors for protein. *J Phys Chem B* 2010;**114**:8574–80.
50. McRae EG, Kasha M. Enhancement of phosphorescence ability upon aggregation of dye molecules. *J Chem Phys* 1958;**28**:721–2.
51. Matsumura Y, Ananthaswamy HN. Toxic effects of ultraviolet radiation on the skin. *Toxicol Appl Pharmacol* 2004;**195**:298–308.
52. D’Orazio J, Jarrett S, Amaro-Ortiz A, Scott T. UV radiation and the skin. *Int J Mol Sci* 2013;**14**:12222–48.
53. Hapuarachchige S, Huang CT, Donnelly MC, Barinka C, Lupold SE, Pomper MG, et al. Cellular delivery of bioorthogonal pretargeting therapeutics in PSMA-positive prostate cancer. *Mol Pharm* 2020;**17**:98–108.
54. Lin F, Chen L, Zhang H, Ching Ngai WS, Zeng X, Lin J, et al. Bioorthogonal prodrug–antibody conjugates for on-target and on-demand chemotherapy. *CCS Chemistry* 2019;**1**:226–36.
55. Wang X, Liu Y, Fan X, Wang J, Ngai WSC, Zhang H, et al. Copper-triggered bioorthogonal cleavage reactions for reversible protein and cell surface modifications. *J Am Chem Soc* 2019;**141**:17133–41.
56. Doronina SO, Toki BE, Torgov MY, Mendelsohn BA, Cerveny CG, Chace DF, et al. Development of potent monoclonal antibody auristatin conjugates for cancer therapy. *Nat Biotechnol* 2003;**21**:778–84.
57. Tobaldi E, Dovgan I, Mosser M, Becht JM, Wagner A. Structural investigation of cyclo-dioxo maleimide cross-linkers for acid and serum stability. *Org Biomol Chem* 2017;**15**:9305–10.
58. Gregson SJ, Masterson LA, Wei B, Pillow TH, Spencer SD, Kang GD, et al. Pyrrolbenzodiazepine dimer antibody–drug conjugates: synthesis and evaluation of noncleavable drug-linkers. *J Med Chem* 2017;**60**:9490–507.
59. Wang Y, Liu L, Fan S, Xiao D, Xie F, Li W, et al. Antibody–drug conjugate using ionized cys-linker-MMAE as the potent payload shows optimal therapeutic safety. *Cancers (Basel)* 2020;**12**:744.
60. Li X, Patterson JT, Sarkar M, Pedzisa L, Kodadek T, Roush WR, et al. Site-specific dual antibody conjugation via engineered cysteine and selenocysteine residues. *Bioconjug Chem* 2015;**26**:2243–8.
61. Lyu Z, Kang L, Buuh ZY, Jiang D, McGuth JC, Du J, et al. A switchable site-specific antibody conjugate. *ACS Chem Biol* 2018;**13**:958–64.
62. Zhou Q. Site-specific antibody conjugation for ADC and beyond. *Biomedicines* 2017;**5**:64.
63. Hamblett KJ, Senter PD, Chace DF, Sun MM, Lenox J, Cerveny CG, et al. Effects of drug loading on the antitumor activity of a monoclonal antibody drug conjugate. *Clin Cancer Res* 2004;**10**:7063–70.
64. Lyon RP, Setter JR, Bovee TD, Doronina SO, Hunter JH, Anderson ME, et al. Self-hydrolyzing maleimides improve the stability and pharmacological properties of antibody–drug conjugates. *Nat Biotechnol* 2014;**32**:1059–62.
65. Christie RJ, Fleming R, Bezabeh B, Woods R, Mao S, Harper J, et al. Stabilization of cysteine-linked antibody drug conjugates with *N*-aryl maleimides. *J Control Release* 2015;**220**:660–70.
66. Fontaine SD, Reid R, Robinson L, Ashley GW, Santi DV. Long-term stabilization of maleimide-thiol conjugates. *Bioconjug Chem* 2015;**26**:145–52.
67. Christie RJ, Tiberghien AC, Du Q, Bezabeh B, Fleming R, Shannon A, et al. Pyrrolbenzodiazepine antibody–drug conjugates designed for stable thiol conjugation. *Antibodies (Basel)* 2017;**6**:20.
68. Shaunak S, Godwin A, Choi JW, Balan S, Pedone E, Vijayarangam D, et al. Site-specific PEGylation of native disulfide bonds in therapeutic proteins. *Nat Chem Biol* 2006;**2**:312–3.

69. Badescu G, Bryant P, Bird M, Henseleit K, Swierkosz J, Parekh V, et al. Bridging disulfides for stable and defined antibody drug conjugates. *Bioconjug Chem* 2014;**25**:1124–36.
70. Huang R, Sheng Y, Wei D, Yu J, Chen H, Jiang B. Bis(vinylsulfonyl) piperazines as efficient linkers for highly homogeneous antibody–drug conjugates. *Eur J Med Chem* 2020;**190**:112080.
71. Sun S, Akkapeddi P, Marques MC, Martinez-Saez N, Torres VM, Cordeiro C, et al. One-pot stapling of interchain disulfides of antibodies using an isobutylene motif. *Org Biomol Chem* 2019;**17**:2005–12.
72. Huang R, Li Z, Sheng Y, Yu J, Wu Y, Zhan Y, et al. *N*-Methyl-*N*-phenylvinylsulfonamides for cysteine-selective conjugation. *Org Lett* 2018;**20**:6526–9.
73. Waalboer DC, Muns JA, Sijbrandi NJ, Schasfoort RB, Haselberg R, Somsen GW, et al. Platinum(II) as bifunctional linker in antibody–drug conjugate formation: coupling of a 4-nitrobenzo-2-oxa-1,3-diazole fluorophore to trastuzumab as a model. *ChemMedChem* 2015;**10**:797–803.
74. Sijbrandi NJ, Merkul E, Muns JA, Waalboer DC, Adamzek K, Bolijn M, et al. A novel platinum(II)-based bifunctional ADC linker benchmarked using 89Zr-desferal and auristatin F-conjugated trastuzumab. *Cancer Res* 2017;**77**:257–67.
75. Merkul E, Muns JA, Sijbrandi NJ, Houthoff HJ, Nijmeijer B, van Rheenen G, et al. An efficient conjugation approach for coupling drugs to native antibodies via the Pt(II) linker *Lx* for improved manufacturability of antibody–drug conjugates. *Angew Chem Int Ed Engl* 2020;**60**:3008–15.
76. Merkul E, Sijbrandi NJ, Muns JA, Aydin I, Adamzek K, Houthoff HJ, et al. First platinum(II)-based metal-organic linker technology (*Lx*) for a plug-and-play development of antibody–drug conjugates (ADCs). *Expert Opin Drug Deliv* 2019;**16**:783–93.
77. Maderna A, Leverett CA. Recent advances in the development of new auristatins: structural modifications and application in antibody drug conjugates. *Mol Pharm* 2015;**12**:1798–812.
78. Burke PJ, Hamilton JZ, Pires TA, Setter JR, Hunter JH, Cochran JH, et al. Development of novel quaternary ammonium linkers for antibody–drug conjugates. *Mol Cancer Ther* 2016;**15**:938–45.
79. Block SS, Stephens RL, Barreto A, Murrill WA. Chemical identification of the Amanita toxin in mushrooms. *Science* 1955;**121**:505–6.
80. Pando O, Dörner S, Preusentanz R, Denkert A, Porzel A, Richter W, et al. First total synthesis of tubulysin B. *Org Lett* 2009;**11**:5567–9.
81. Quintieri L, Geroni C, Fantin M, Battaglia R, Rosato A, Speed W, et al. Formation and antitumor activity of PNU-159682, a major metabolite of nemorubicin in human liver microsomes. *Clin Cancer Res* 2005;**11**:1608–17.
82. Park S, Kim SY, Cho J, Jung D, Seo D, Lee J, et al. Aryl sulfate is a useful motif for conjugating and releasing phenolic molecules: sulfur fluorine exchange click chemistry enables discovery of *ortho*-hydroxy-protected aryl sulfate linker. *Bioconjug Chem* 2019;**30**:1957–68.
83. Han TH, Zhao B. Absorption, distribution, metabolism, and excretion considerations for the development of antibody–drug conjugates. *Drug Metab Dispos* 2014;**42**:1914–20.
84. Lyon RP, Bovee TD, Doronina SO, Burke PJ, Hunter JH, Neff-LaFord HD, et al. Reducing hydrophobicity of homogeneous antibody–drug conjugates improves pharmacokinetics and therapeutic index. *Nat Biotechnol* 2015;**33**:733–5.
85. Sun X, Ponte JF, Yoder NC, Laleau R, Coccia J, Lanieri L, et al. Effects of drug-antibody ratio on pharmacokinetics, biodistribution, efficacy, and tolerability of antibody–maytansinoid conjugates. *Bioconjug Chem* 2017;**28**:1371–81.
86. Abrahams CL, Li X, Embry M, Yu A, Krimm S, Krueger S, et al. Targeting CD74 in multiple myeloma with the novel, site-specific antibody–drug conjugate STRO-001. *Oncotarget* 2018;**9**:37700–14.
87. Shao S, Tsai MH, Lu J, Yu T, Jin J, Xiao D, et al. Site-specific and hydrophilic ADCs through disulfide-bridged linker and branched PEG. *Bioorg Med Chem Lett* 2018;**28**:1363–70.
88. Zhao RY, Wilhelm SD, Audette C, Jones G, Leece BA, Lazar AC, et al. Synthesis and evaluation of hydrophilic linkers for antibody–maytansinoid conjugates. *J Med Chem* 2011;**54**:3606–23.
89. Walker JA, Sorkin MR, Ledesma F, Kabaria SR, Barfield RM, Rabuka D, et al. Hydrophilic sequence-defined cross-linkers for antibody–drug conjugates. *Bioconjug Chem* 2019;**30**:2982–8.
90. Simmons JK, Burke PJ, Cochran JH, Pittman PG, Lyon RP. Reducing the antigen-independent toxicity of antibody–drug conjugates by minimizing their non-specific clearance through PEGylation. *Toxicol Appl Pharmacol* 2020;**392**:114932.
91. Viricel W, Fournet G, Beaumel S, Perrial E, Papot S, Dumontet C, et al. Monodisperse polysarcosine-based highly-loaded antibody–drug conjugates. *Chem Sci* 2019;**10**:4048–53.
92. Zhang D, Yu SF, Ma Y, Xu K, Dragovich PS, Pillow TH, et al. Chemical structure and concentration of intratumor catabolites determine efficacy of antibody drug conjugates. *Drug Metab Dispos* 2016;**44**:1517–23.
93. Zhang D, Yu SF, Khojasteh SC, Ma Y, Pillow TH, Sadowsky JD, et al. Intratumoral payload concentration correlates with the activity of antibody–drug conjugates. *Mol Cancer Ther* 2018;**17**:677–85.
94. Zhang D, Dragovich PS, Yu SF, Ma Y, Pillow TH, Sadowsky JD, et al. Exposure-efficacy analysis of antibody–drug conjugates delivering an excessive level of payload to tissues. *Drug Metab Dispos* 2019;**47**:1146–55.
95. Sharkey RM, McBride WJ, Cardillo TM, Govindan SV, Wang Y, Rossi EA, et al. Enhanced delivery of SN-38 to human tumor xenografts with an anti-Trop-2-SN-38 antibody conjugate (sacituzumab govitecan). *Clin Cancer Res* 2015;**21**:5131–8.
96. Mullard A. Maturing antibody–drug conjugate pipeline hits 30. *Nat Rev Drug Discov* 2013;**12**:329–32.
97. Younes A, Bartlett NL, Leonard JP, Kennedy DA, Lynch CM, Sievers EL, et al. Brentuximab vedotin (SGN-35) for relapsed CD30-positive lymphomas. *N Engl J Med* 2010;**363**:1812–21.
98. Krop IE, Beeram M, Modi S, Jones SF, Holden SN, Yu W, et al. Phase I study of trastuzumab-DM1, an HER2 antibody–drug conjugate, given every 3 weeks to patients with HER2-positive metastatic breast cancer. *J Clin Oncol* 2010;**28**:2698–704.